Mark Collard and Nickolas Franchino
Department of Anthropology, University College London, Gower Street, London, WC1E 6BT, U.K.
Tel: 011 44 20 7679 2367; Fax: 011 44 20 7679 7728;
E-mail for MC: m.collard@ucl.ac.uk
E-mail for NF: darwinsfoot@hotmail.com

Received 28 January 2002
Revision received 21 May 2002 and accepted 22 May 2002

Keywords: modern human origins, pairwise difference analysis, hominoid, primate, hominid, craniodental, soft tissue, morphology.

Pairwise difference analysis in modern human origins research

Pairwise difference analysis is a phenetic method that groups taxa on the basis of the number of differences they exhibit. Recently, pairwise difference analysis has been used to investigate the phylogenetic relationships of hominid fossils at the centre of the modern human origins debate. It has been argued that the results of these analyses disprove the African replacement model of modern human origins, and support instead its competitor, the multiregional evolution model. However, this inference is problematic because the ability of pairwise difference analysis to recover phylogenetic information from morphological data has not been demonstrated. With this in mind, we conducted pairwise difference analyses of craniodental and soft tissue evidence from a group of extant primates for which a reliable molecular phylogeny is available, the hominoids. We found that the phylogenies yielded by the pairwise difference analyses were incompatible with the molecular phylogeny for the group. Given the robustness of the molecular phylogeny, these results suggest that pairwise difference analysis cannot be relied on to generate reliable estimates of primate phylogeny from morphological data. The corollary of this is that the results of published pairwise difference analyses of hominid fossils are not informative regarding the origin of modern humans.

Journal of Human Evolution (2002) **43,** 323–352
doi:10.1006/jhev.2002.0578
Available online at http://www.idealibrary.com on IDEAL®

Introduction

The emergence of modern humans has been the focus of considerable debate over the last 30 years (e.g., Howells, 1973; Thorne & Wolpoff, 1981, 1992; Cann *et al.*, 1987; Braüer, 1992; Smith *et al.*, 1989; Stringer, 1989, 1992, 2001; Wolpoff, 1989, 1992; Maddison, 1991; Aiello, 1993; Lahr, 1994; Lieberman, 1995; Hublin *et al.*, 1996; Braüer & Stringer, 1997; Krings *et al.*, 1997; Churchill & Smith, 2000; McBrearty & Brooks, 2000; Wolpoff *et al.*, 2000, 2001; Clark, 2002). Currently, three models dominate the dispute: the African replacement model, the assimilation model, and the multiregional evolution model (Churchill & Smith, 2000; Stringer, 2001). The African replacement model contends that modern humans arose in Africa around 150 ka and spread from there throughout the rest of the world replacing local archaic hominids with minimal interbreeding (e.g., Stringer & Andrews, 1988; Stringer, 1989, 1992; Braüer, 1992; Braüer & Stringer, 1997). The assimilation model also posits a recent African origin for modern humans, but unlike the African replacement model it contends that regional groups of archaic hominids, such as the Neanderthals, made a significant contribution to the gene pool of living humans (Smith *et al.*, 1989; Churchill & Smith, 2000). The multiregional evolution model is still further removed from the African replacement model. It avers that modern humans arose from archaic hominids in several areas of the Old World by way of a process of genetic exchange and local selection that operated throughout the whole of the Pleistocene (e.g., Thorne &

0047–2484/02/030323+30$35.00/0

Wolpoff, 1981, 1992; Wolpoff, 1989, 1992; Frayer *et al.*, 1993; Wolpoff *et al.*, 2000). Thus, the multiregional evolution model not only argues that nonAfrican archaic hominids made a significant contribution to the gene pool of living humans, but also discounts migration of recently evolved Africans as a significant factor in the emergence of modern humans outside of Africa.

Of the predictions that can be derived from the recent African origin, assimilation and multiregional evolution models, perhaps the most important concern the phylogenetic relationships of the nonAfrican early modern humans. The African replacement model predicts that European, East Asian and Australasian early modern humans are more closely related to African early modern humans than they are to archaic humans in Europe, East Asia and South East Asia, respectively. The assimilation model also predicts that early modern humans from Eurasia and Australasia are most closely related to African early modern humans, but it anticipates some evidence for ancestor-descendant relationships between early modern and archaic humans outside of Africa. In contrast, the multiregional evolution model predicts that early modern humans in Europe, East Asia and Australasia are at least as closely related to European, East Asian and South East Asian archaic humans, respectively, as they are to African early modern humans.

To test these predictions, hominid palaeontologists have recently turned to a form of analysis that is used in molecular biology to address phylogenetic problems, pairwise difference analysis (Hawks *et al.*, 2000; Kramer *et al.*, 2001; Wolpoff *et al.*, 2001). Pairwise difference analysis is a phenetic method that groups taxa on the basis of the number of differences they exhibit. It assumes that all taxa are related, that each difference between a pair of taxa represents a mutation, and that mutations occur at a constant rate through time. Thus, in pairwise difference analysis taxa that exhibit few differences are deemed to be more closely related than taxa that exhibit many differences because they must share a common ancestor that lived more recently. Pairwise difference analysis is widely used in molecular biology since it underpins the molecular clock (Hedrick, 2000). Pairwise difference analysis has also been applied to ancient DNA sequences in order to investigate the affinities of Neanderthal and modern human fossils (e.g., Krings *et al.*, 1997, 1999; Ovchinnikov *et al.*, 2000). Palaeoanthropological applications of pairwise difference analysis have focused on the number of differences between pairs of fossil specimens, and on the mean number of differences among groups of fossil specimens (Hawks *et al.*, 2000; Kramer *et al.*, 2001; Wolpoff *et al.*, 2001). This is similar to the approach adopted in molecular clock applications of pairwise difference analysis, and differs from the approach adopted in pairwise difference analyses of ancient DNA. In the latter, the phylogenetic relationships of an ancient individual are assessed relative to the frequency distribution of the number of differences between all possible pairs of individuals in a large sample of extant individuals (e.g., Krings *et al.*, 1997, 1999; Ovchinnikov *et al.*, 2000).

Applications of pairwise difference analysis in palaeoanthropology have focused on fossils from Australia, Europe and South West Asia (Hawks *et al.*, 2000; Kramer *et al.*, 2001; Wolpoff *et al.*, 2001). Hawks *et al.* (2000) used pairwise difference analysis to investigate the affinities of WLH-50, a modern human fossil from the Willandra Lakes area of Australia that dates to 15–13 ka. Using 16 qualitative cranial characters, they compared WLH-50 with 10 Late Pleistocene modern human fossils from Africa and South West Asia, and seven specimens from the Javanese site of Ngandong that are Pleistocene in date, and which are usually classified as *Homo erectus* (e.g., Rightmire, 1990). The comparisons

revealed that WLH-50 is closer to six of the seven specimens from Ngandong than to any other specimen, and is only separated from the seventh Ngandong specimen by one South West Asian specimen (Skhul 9). Hawks *et al.* (2000) inferred from this that WLH-50 is likely to be a descendant of all three groups, and that the African replacement model of modern human origins can therefore be discounted. Kramer *et al.* (2001) used pairwise difference analysis of 12 qualitative cranial characters to assess the phylogenetic status of Neanderthal and early modern human fossils from South West Asia. Specifically, they tested the prediction from the African replacement model that the Neanderthal specimens from Tabun and Amud should group together to the exclusion of the modern human specimens from Skhul and Qafzeh. Kramer *et al.* (2001) found that the prediction was not met. The mean number of differences between Tabun and the Skhul/Qafzeh crania did not differ significantly from the number of differences between Tabun and Amud. They concluded from this that the African replacement model can be discounted. Wolpoff *et al.* (2001) replicated the WLH-50 analysis carried out by Hawks *et al.* (2000) and also outlined a pairwise difference analysis that focused on the affinities of early modern human fossils from the Moravian Upper Palaeolithic site of Mladec. Based on 30 qualitative cranial characters, the latter analysis indicated that the number of differences between the Mladec crania and Neanderthal specimens from Europe and South West Asia was similar to the number of differences between the Mladec crania and early modern human specimens from South West Asia. Wolpoff *et al.* (2001) argued that the results of their pairwise difference analyses are in line with the multiregional evolution model of modern human origins rather than the African replacement model.

The studies in which pairwise difference analysis has been applied to hominid fossil material appear to refute the African replacement model of modern human origins and support instead its competitor, the multiregional evolution model (Hawks *et al.*, 2000; Kramer *et al.*, 2001; Wolpoff *et al.*, 2001). However, while the ability of pairwise difference analysis to recover phylogenetic information from biomolecular data is well established, its ability to recover such information from morphological data has not been evaluated. As such, the inference that the pairwise difference analyses of fossil hominids undercut the African replacement model and confirm the multiregional evolution model is problematic. The results of these analyses may, as Hawks *et al.* (2000), Kramer *et al.* (2001) and Wolpoff *et al.* (2001) contend, disprove the African replacement model and support the multiregional evolution model. But it is also possible that pairwise difference analysis is unable to recover phylogenetic information from morphological data, in which case the results of the fossil hominid analyses are uninformative regarding the African replacement and multiregional evolution models of modern human origins.

Here we report a study in which the ability of pairwise difference analysis to recover phylogenetic information from hominid morphological data was evaluated through analyses of craniodental and soft tissue evidence from the extant hominoids. These primates have been the focus of considerable molecular phylogenetic research, and there is now widespread agreement that their phylogenetic relationships can be considered known (e.g., Ruvolo, 1997; Gagneux & Varki, 2001; Page & Goodman, 2001). Accordingly we assumed that, if the phylogenetic hypotheses yielded by pairwise difference analyses of the hominoid morphological data match the group's molecular phylogeny (Figure 1), pairwise difference analysis can be relied on to recover phylogenetic information from primate morphological data, and the results of Hawks *et al.*'s

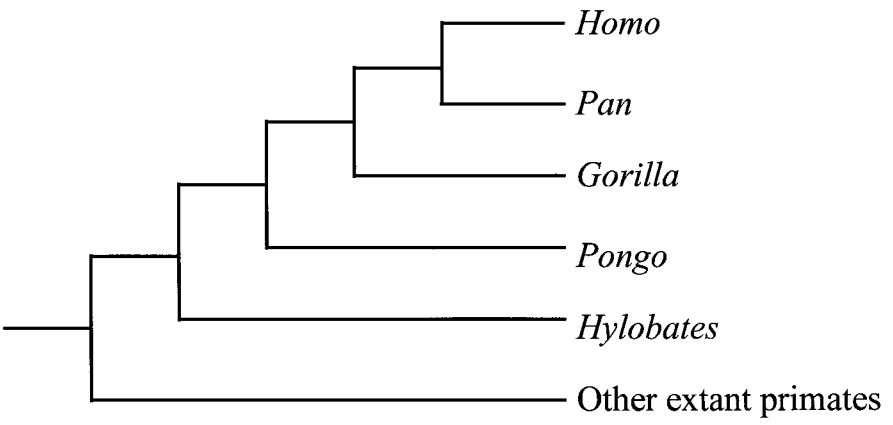

Figure 1. Hominoid molecular phylogeny.

(2000), Kramer *et al.*'s (2001) and Wolpoff *et al.*'s (2001) pairwise difference analyses of fossil hominids can be considered valid. Conversely, we also assumed that, if pairwise difference analyses of the hominoid morphological data yield phylogenetic hypotheses that disagree with the group's molecular phylogeny, pairwise difference analysis cannot be relied on to recover phylogenetic information from primate morphological data, and the results of Hawks *et al.*'s (2000), Kramer *et al.*'s (2001) and Wolpoff *et al.*'s (2001) fossil hominid pairwise difference analyses cannot be considered valid.

Materials and methods

Three datasets were employed in the study. The first comprised the states of 96 qualitative craniodental characters recorded on *Gorilla*, *Homo*, *Hylobates*, *Pan* and *Pongo*. This dataset was taken from Collard & Wood (2000). The character definitions and states are given in Appendix 1. The second dataset comprised the states of 171 qualitative soft tissue characters recorded on *Gorilla*, *Homo*, *Hylobates*, *Pan* and *Pongo*. These data were taken from Gibbs *et al.* (2002). The definitions and states of the characters are given in Appendix 2. The third dataset consisted of values for 129 craniodental measurements recorded on mixed sex samples of adult *Colobus*, *Gorilla*, *Homo*, *Pan* and *Pongo*. Seventy-seven of the measurements were recorded on 37 *Gorilla gorilla* (20 males, 17 females), 75 *H. sapiens* (40 males, 35 females), 35 *Pan troglodytes* (13 males, 22 females), 41 *Pongo pygmaeus* (20 males, 21 females) and 24 *Colobus guereza* (12 males, 12 females). The other 52 measurements were recorded on 20 *G. gorilla* (ten males, ten females), 20 *H. sapiens* (ten males, ten females), 20 *P. troglodytes* (ten males, ten females), 20 *P. pygmaeus* (ten males, ten females) and 20 *C. guereza* (ten males, ten females). These data were also taken from Collard & Wood (2000). Details of the measurements are given in Appendix 3. Cranial measurements were rounded up to the nearest 1 mm, and dental measurements to the nearest 0.1 mm.

Four analyses were carried out to assess the ability of pairwise difference analysis to recover phylogenetic information from primate morphological data. The first and second analyses involved the qualitative craniodental and soft tissue datasets, respectively. In both analyses, the states exhibited by the taxa were compared on a pairwise basis and the number of differences

between each pair recorded in a matrix. Thereafter, a nearest-neighbour phylogeny was constructed from the matrix of differences by sequentially linking taxa that returned the smallest number of differences in the pairwise comparisons. This method of clustering was chosen as it best approximates the procedure used by Hawks *et al.* (2000), Kramer *et al.* (2001) and Wolpoff *et al.* (2001). Lastly, the morphological phylogeny was judged against the consensus molecular phylogeny for the extant hominoids, which was assumed to accurately represent the relationships among them (Ruvolo, 1997; Gagneux & Varki, 2001; Page & Goodman, 2001). The third analysis focussed on the quantitative craniodental data. The data were adjusted to counteract the confounding effects of the size differences among the taxa. This was accomplished by dividing each value by the geometric mean of all the values for the appropriate specimen (Darroch & Mosiman, 1985; Jungers *et al.*, 1995). Next, the significance of the differences between the means was evaluated on a pairwise basis using the two-tailed *t*-test, and the number of significant differences recorded in a matrix. Subsequently, a nearest neighbour phylogeny was constructed and then judged against the hominoid molecular phylogeny. In the fourth analysis, the 96-character qualitative craniodental and 171-character soft tissue datasets were combined. Next, the states exhibited by the taxa were compared on a pairwise basis and the number of differences between each pair recorded in a matrix. Thereafter, a nearest neighbour phylogeny was constructed and then judged against the hominoid molecular phylogeny. Lastly, the effect of the small number of uncertain and polymorphic character states in the first two datasets was assessed. This was accomplished by comparing the results of analyses in which the ambiguous character states were set to 0 with the results of analyses in which the ambiguous character states were set to 1. All the analyses were performed in *Excel 2001*.

Table 1 Results of pairwise difference analysis of hominoid qualitative craniodental dataset

	Homo	*Hylobates*	*Pan*	*Pongo*
Gorilla	53	58	20	62
Homo		58	42	64
Hylobates			58	68
Pan				63

Each value represents the number of morphological differences between a pair of taxa.

Results

Four analyses were conducted in order to assess the ability of pairwise difference analysis to recover phylogenetic information from primate morphological data. In the first analysis, pairwise difference analysis was applied to a dataset comprising the states of 96 qualitative characters recorded on *Gorilla*, *Homo*, *Hylobates*, *Pan* and *Pongo*. The number of differences among the taxa is presented in Table 1, and the phylogeny derived from the number of differences is shown in Figure 2. The latter is incompatible with the hominoid molecular phylogeny (Figure 1), since it suggests that *Gorilla* and *Pan* share a common ancestor to the exclusion of *Homo*, *Hylobates* and *Pongo*. It also differs from the molecular phylogeny in suggesting that *Gorilla*, *Homo* and *Pan* share an ancestor to the exclusion of *Hylobates* and *Pongo*, and that *Gorilla*, *Homo*, *Hylobates* and *Pan* share an ancestor to the exclusion of *Pongo*. The analyses conducted to examine the effects of the uncertain and polymorphic character states (characters 63, 64, 85 and 94) produced phylogenies with the same topology as the phylogeny obtained in the analysis of the unaltered data. The first analysis therefore suggested that pairwise difference analysis is unable to recover

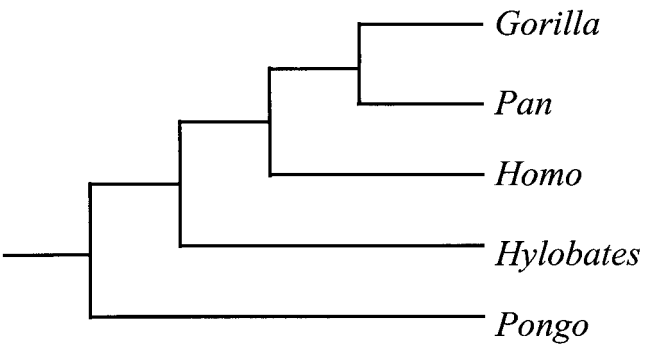

Figure 2. Phylogeny returned by pairwise difference analysis of 96 qualitative craniodental characters.

Table 2 Results of pairwise difference analysis of soft tissue dataset

	Homo	*Hylobates*	*Pan*	*Pongo*
Gorilla	107	99	100	108
Homo		121	92	123
Hylobates			132	98
Pan				115

Each value represents the number of morphological differences between a pair of taxa.

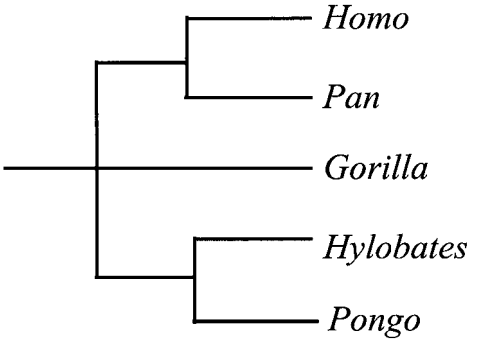

Figure 3. Phylogeny returned by pairwise difference analysis of 171 soft tissue characters.

phylogenetic information from primate morphological data.

In the second analysis, pairwise difference analysis was applied to a dataset consisting of the states of 171 qualitative soft tissue characters recorded on *Gorilla*, *Homo*, *Hylobates*, *Pan* and *Pongo*. Table 2 shows the number of differences among the taxa, and Figure 3 presents the phylogeny derived from the number of differences. The phylogeny is consistent with the hominoid molecular phylogeny (Figure 1) in that it suggests that *Homo* and *Pan* share a common ancestor to the exclusion of *Gorilla*, *Hylobates* and *Pongo*. However, it differs from the molecular phylogeny in suggesting that *Hylobates* and *Pongo* share an ancestor to the exclusion of *Gorilla*, *Homo* and *Pan*. It also differs from the molecular phylogeny in suggesting that *Gorilla* is equally closely related to the (*Homo*, *Pan*) clade and the (*Hylobates*, *Pongo*) clade. One of the analyses undertaken to assess the effect of the missing state for *Hylobates* for character 18 returned a phylogeny with the same topology as the unaltered data. The other analysis returned a phylogeny that was even more incongruent with the molecular phylogeny. It suggested that *Hylobates* and *Pongo* share an ancestor to the exclusion of *Gorilla*, *Homo* and *Pan*, that *Gorilla* shares an ancestor with *Hylobates* and *Pongo* to the exclusion of *Homo* and *Pan*, and that *Homo* and *Pan* share an ancestor to the exclusion of *Gorilla*, *Hylobates* and *Pongo*. Hence, the second analysis also suggested that pairwise difference analysis is unable to recover phylogenetic information from primate morphological data.

In the third analysis, pairwise difference analysis was applied to a dataset consisting of the states of 129 quantitative craniodental

Table 3 Results of pairwise difference analysis of quantitative craniodental dataset

	Pongo	*Gorilla*	*Pan*	*Homo*
Colobus	118	121	111	114
Pongo		95	86	124
Gorilla			104	121
Pan				119

Each value represents the number of morphological differences between a pair of taxa.

characters recorded on *Colobus*, *Gorilla*, *Homo*, *Pan* and *Pongo*. The number of differences among the taxa is shown in Table 3, and the phylogeny derived from the number of differences is presented in Figure 4. The phylogeny differs considerably from the molecular phylogeny (Figure 1). Most notably it suggests that the Old World monkey genus *Colobus* shares a common ancestor with three of the hominoid genera, *Gorilla*, *Pan* and *Pongo*, to the exclusion of the fourth hominoid genus, *Homo*. In addition, the craniometric phylogeny suggests that *Pan* and *Pongo* share a common ancestor to the exclusion of *Gorilla*. Thus, the third analysis, like the previous two analyses, suggests pairwise difference analysis is unable to recover phylogenetic information from primate morphological data.

In the fourth analysis, we combined the 96-character craniodental and the 171-character soft tissue datasets, subjected the combined data set to pairwise difference analysis, and then compared the resulting phylogeny with the hominoid molecular phylogeny. The number of differences between the taxa is shown in Table 4, and the phylogeny derived from the number of differences is presented in Figure 5. The phylogeny obtained from the combined dataset had the same topology as the phylogeny obtained when the qualitative craniodental data were analysed independently. In contrast to the molecular phylogeny (Figure 1), it suggested that *Gorilla* and *Pan* share a common ancestor to the exclusion of *Homo*, *Hylobates* and *Pongo*, that *Gorilla*, *Homo* and *Pan* share an ancestor to the exclusion of *Hylobates* and *Pongo*, and that *Gorilla*, *Homo*, *Hylobates* and *Pan* share an ancestor to the exclusion of *Pongo*. Therefore, the fourth analysis agreed with the other three analyses in suggesting that pairwise difference analysis is unable to recover phylogenetic information from primate morphological data.

Discussion

In order to assess the ability of pairwise difference analysis to recover phylogenetic information from primate morphological data, four analyses were carried out. In each analysis, pairwise difference analysis was applied to a hominoid morphological dataset, a nearest-neighbour phylogeny was constructed from the results of the pairwise difference analysis, and then the morphological phylogeny was judged against the group's molecular phylogeny. In all four analyses the phylogenetic hypotheses returned by pairwise difference analysis were incompatible with the molecular phylogeny for the extant hominoids.

Given the robustness of the hominoid molecular phylogeny (Ruvolo, 1997; Gagneux & Varki, 2001; Page & Goodman, 2001), these results indicate that pairwise difference analysis cannot be relied on to recover phylogenetic information from primate morphological datasets. It is possible that future studies will show that pairwise difference analysis is able to recover phylogenetic information from some datasets, but the results of our analyses indicate that it is unable to recover phylogenetic information from all primate morphological datasets. Thus, it cannot automatically be assumed that a phylogeny yielded by a pairwise difference analysis of primate morphological data is accurate. The corollary of this is that the results of the pairwise difference analyses

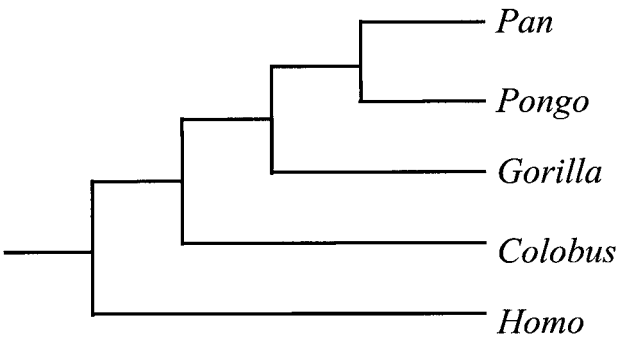

Figure 4. Phylogeny returned by pairwise difference analysis of 129 quantitative craniodental characters.

Table 4 Results of pairwise difference analysis of qualitative craniodental and soft tissue dataset

	Homo	*Hylobates*	*Pan*	*Pongo*
Gorilla	160	157	120	170
Homo		179	134	187
Hylobates			190	166
Pan				178

Each value represents the number of morphological differences between a pair of taxa.

of fossil hominids carried out by Hawks *et al.* (2000), Kramer *et al.* (2001) and Wolpoff *et al.* (2001) are uninformative regarding modern human origins. They may refute the African replacement model and support the multiregional evolution model, as Hawks *et al.* (2000), Kramer *et al.* (2001) and Wolpoff *et al.* (2001) contend, but it may also be the case that, like the phylogenetic hypotheses we obtained using pairwise difference analysis, the fossil hominid phylogenetic hypotheses are inaccurate. Since there is no way of determining which of these possibilities is correct, the results of Hawks *et al.*'s (2000), Kramer *et al.*'s (2001) and Wolpoff *et al.*'s (2001) pairwise difference analyses neither refute the African replacement nor support the multiregional evolution model.

Three potential criticisms of our analyses could undermine the foregoing conclusions regarding the reliability of pairwise difference analysis of primate morphological data, and the implications of the results of the fossil hominid pairwise difference analyses carried out by Hawks *et al.* (2000), Kramer *et al.* (2001) and Wolpoff *et al.* (2001). The first is that our analyses focused on the phylogenetic relationships among genera whereas the fossil hominid analyses concentrated on the phylogenetic relationships among individual fossils and groups of fossils. Thus, it could be argued that it is inappropriate to conclude from our results that published pairwise difference analyses of fossil hominids are incapable of refuting or supporting models of modern human origins. This criticism would perhaps be valid if the ease with which phylogenetic relationships can be reconstructed were inversely correlated with taxonomic level. But this does not seem to be the case. On the contrary, it is widely assumed that intraspecific phylogenetic relationships are more difficult to reconstruct than interspecific phylogenetic relationships, which in turn are more difficult to reconstruct than the phylogenetic relationships among supraspecific taxa (e.g., Trinkaus, 1990, 1992; Lieberman, 1995; Collard & Wood, 2000). As such, we believe the results of our analyses are relevant to the reliability of the results of published fossil hominid pairwise difference analyses.

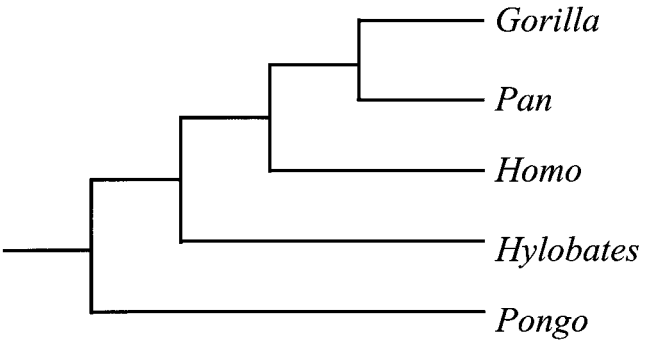

Figure 5. Phylogeny returned by pairwise difference analysis of 96 qualitative craniodental and 171 soft tissue characters.

The second potential criticism concerns the type of morphological data employed in our analyses. It has been suggested recently that craniodental characters are unreliable for reconstructing the phylogenetic relationships among higher primate species and genera (Hartman, 1988; Harrison, 1993; Pilbeam, 1996; Collard & Wood, 2000). Thus, it could be argued that the incongruence between our morphological phylogenies and the molecular phylogeny reflect the limitations of the data rather than the limitations of pairwise difference analysis. However, this argument cannot be sustained. Gibbs and colleagues' (2000, 2002) cladistic analyses of the hominoid soft tissue dataset we employed yielded a well-supported phylogeny with the same topology as the hominoid molecular phylogeny (Figure 1). In contrast, the pairwise difference analysis of the data reported here returned a phylogeny that disagrees with the hominoid molecular phylogeny regarding the relationships of *Gorilla*, *Hylobates* and *Pongo* (Figure 3). This strongly supports the inference that pairwise difference analysis is not useful for estimating phylogenetic relationships among primate species and genera. Moreover, even if it is assumed that the results of the analyses in which pairwise difference analysis was applied to hominoid craniodental data reflect the limitations of such data, there is still no reason to consider the results of the pairwise difference analyses carried out by Hawks *et al.* (2000), Kramer *et al.* (2001) and Wolpoff *et al.* (2001) to be informative regarding modern human origins, since they are also based on higher primate craniodental characteristics.

The third potential criticism is that our datasets are inadequate as far as sample size and character number are concerned. We reject this criticism on two counts, especially as it relates to our conclusion that the results of the pairwise difference analyses carried out by Hawks *et al.* (2000), Kramer *et al.* (2001) and Wolpoff *et al.* (2001) are incapable of refuting or supporting any model of modern human origins. First, we used many more characters than Hawks *et al.* (2000), Kramer *et al.* (2001) and Wolpoff *et al.* (2001). We employed between 96 and 267 characters, while Hawks *et al.* (2000) used 16, Kramer *et al.* (2001) used 12, and Wolpoff *et al.* (2001) used 30. Second, while our qualitative datasets are based on observations of relatively small numbers of individuals (Collard & Wood, 2000; Gibbs *et al.*, 2002), our quantitative data are derived from samples of specimens that are considerably larger than those employed by Hawks *et al.* (2000), Kramer *et al.* (2001) and Wolpoff *et al.* (2001) in their fossil hominid pairwise difference analyses. Our quantitative dataset comprises values for between 20 and 75 specimens per genus,

whereas the datasets employed by Hawks *et al.* (2000), Kramer *et al.* (2001) and Wolpoff *et al.* (2001) include information on 36 specimens in total. It is possible that the number of characters and individuals we employed are insufficient for pairwise difference analysis to be able recover the correct phylogeny. However, if our results are problematic due to an insufficient number of characters and/or number of specimens having been examined, the same must hold for the results of Hawks *et al.* (2000), Kramer *et al.* (2001) and Wolpoff *et al.* (2001), in which case our conclusion that the latter are uninformative regarding modern human origins still stands.

Thus, the potential criticisms of our study can either be discounted or shown to be less significant in relation to our analyses than to the pairwise difference analyses of fossil hominids conducted by Hawks *et al.* (2000), Kramer *et al.* (2001) and Wolpoff *et al.* (2001). We believe, therefore, that there is no reason to reject the conclusion that pairwise difference analysis cannot be relied on to recover phylogenetic information from primate morphological datasets. We also believe that there is no reason to reject the conclusion that the results of the pairwise difference analyses of fossil hominids carried out by Hawks *et al.* (2000), Kramer *et al.* (2001) and Wolpoff *et al.* (2001) are uninformative regarding modern human origins. It is important to note that these conclusions do not lend support to any model of modern human origins. It does not follow from the failure of our analyses to support the conclusions of Hawks *et al.* (2000), Kramer *et al.* (2001) and Wolpoff *et al.* (2001) that the African replacement model is correct and the multiregional evolution model incorrect. Rather the results of our analyses simply mean that the merits of the African replacement and multiregional evolution models of modern human origins should be assessed without reference to Hawks *et al.*'s (2000), Kramer *et al.*'s (2001) and Wolpoff *et al.*'s (2001) pairwise difference analyses of fossil hominids.

Conclusions

In this study we sought to evaluate recent claims that pairwise difference analyses of hominid fossils disprove the African replacement model of modern human origins, and support instead its competitor, the multiregional evolution model (Hawks *et al.*, 2000; Kramer *et al.*, 2001; Wolpoff *et al.*, 2001). To do so, we conducted four pairwise difference analyses of craniodental and morphological data from a group of extant primates for which a reliable molecular phylogeny is available, the hominoids. In each analysis, pairwise difference analysis was applied to a morphological dataset, a phylogeny was constructed by sequentially linking taxa that returned the smallest number of differences in the pairwise difference analysis, and then the morphological phylogeny was judged against the group's molecular phylogeny. In all four analyses the phylogenetic hypotheses returned by pairwise difference analysis were incompatible with the molecular phylogeny for the extant hominoids.

Given the robustness of the hominoid molecular phylogeny, the results of our analyses indicate that pairwise difference analysis cannot be relied on to recover phylogenetic information from all primate morphological datasets. The corollary of this is that the results of the pairwise difference analyses of fossil hominids carried out by Hawks *et al.* (2000), Kramer *et al.* (2001) and Wolpoff *et al.* (2001) are incapable of refuting or supporting any model of modern human origins. Thus, contrary to the claims of Hawks *et al.* (2000), Kramer *et al.* (2001) and Wolpoff *et al.* (2001), the results of their pairwise difference analyses of fossil hominids do not refute the African replacement model and support the multiregional evolution model.

Acknowledgements

We thank Nicole Silverman and Chris Stringer for their assistance with this paper. We also thank the following institutions for providing access to specimens in their care: the Natural History Museum, London, the Anthropologisches Institut und Museum, Universität Zürich-Irchel, Zurich, the Muséum d'Histoire Naturelle, Genève, the Muséum d'Histoire Naturelle, Paris, and the Museum für Naturkunde, Humboldt-Universitat zu Berlin, Berlin.

References

Aiello, L. C. (1993). The fossil evidence for the origins of modern humans. *Am. Anthrop.* **95,** 73–96.

Braüer, G. (1992). Africa's place in the evolution of *Homo sapiens*. In (G. Braüer & F. H. Smith, Eds) *Continuity or Replacement? Controversies in* Homo sapiens *Evolution*, pp. 83–98. Rotterdam: Balkema.

Braüer, G. & Stringer, C. B. (1997). Models, polarization, and perspectives on modern human origins. In (G. A. Clark & C. Willermet, Eds) *Conceptual Issues in Modern Human Origins Research*, pp. 191–201. New York: Aldine de Gruyter.

Cann, R. L., Stoneking, M. & Wilson, A. C. (1987). Mitochondrial DNA and human evolution. *Nature* **329,** 111–112.

Clark, G. A. (2002). Neandertal archaeology—implications for our origins. *Am. Anthrop.* **104,** 50–67.

Churchill, S. E. & Smith, F. (2000). Makers of the early Aurignacian of Europe. *Yearb. Phys. Anthrop.* **43,** 61–115.

Collard, M. & Wood, B. A. (2000). How reliable are human phylogenetic hypotheses? *Proc. natn. Acad. Sci. USA* **97,** 5003–5006.

Darroch, J. N. & Mosiman, J. E. (1985). Canonical and principal components of shape. *Biometrika* **72,** 241–252.

Frayer, D., Wolpoff, M., Smith, F., Thorne, A. & Pope, G. (1993). The fossil evidence for modern human origins. *Am. Anthrop.* **95,** 14–50.

Gagneux, P. & Varki, A. (2001). Genetic differences between humans and great apes. *Mol. Phylogenet. Evol.* **18,** 2–13.

Gibbs, S., Collard, M. & Wood, B. A. (2000). Soft-tissue characters in higher primate phylogenetics. *Proc. natn. Acad. Sci. USA* **97,** 11130–11132.

Gibbs, S., Collard, M. & Wood, B. A. (2002). Soft tissue anatomy of the extant hominoids: a review and phylogenetic analysis. *J. Anat.* **200,** 3–49.

Harrison, T. (1993). Cladistic concepts and the species problem in hominoid evolution. In (W. H. Kimbel & L. B. Martin, Eds) *Species, Species Concepts and Primate Evolution*, pp. 345–371. New York: Plenum Press.

Hartman, S. E. (1988). A cladistic analysis of hominoid molars. *J. hum. Evol.* **17,** 489–502.

Hawks, J., Oh, S., Hunley, K., Dobson, S., Cabana, G., Dayalu, P. & Wolpoff, M. H. (2000). An Australasian test of the recent African origin theory using the WLH-50 calvarium. *J. hum. Evol.* **39,** 1–22.

Heddrick, P. W. (2000). *Genetics of Populations*. Sudbury, MA: Jones & Bartlett.

Howells, W. W. (1973). *Evolution of the Genus* Homo. Reading: Addison-Wesley.

Hublin, J.-J., Spoor, F., Braun, M., Zonneveld, F. & Condemi, S. (1996). A late Neanderthal associated with Upper Palaeolithic artefacts. *Nature* **381,** 224–226.

Jungers, W. L., Falsetti, A. B. & Wall, C. E. (1995). Shape, relative size, and size-adjustments in morphometrics. *Yearb. phys. Anthrop.* **38,** 137–161.

Kramer, A., Crummett, T. L. & Wolpoff, M. H. (2001). Out of Africa and into the Levant: replacement or admixture in Western Asia. *Quatern. Int.* **75,** 51–63.

Krings, M., Geisert, H., Schmitz, R. W., Krainitzki, H. & Pääbo, S. (1999). DNA sequence of the mitochondrial hypervariable region II from the Neanderthal type specimen. *Proc. natn. Acad. Sci. USA* **96,** 5581–5585.

Krings, M., Stone, A., Schmitz, R. W., Krainitzki, H., Stoneking, M. & Pääbo, S. (1997). Neanderthal DNA sequences and the origin of modern humans. *Cell* **90,** 19–30.

Lahr, M. M. (1994). The Multiregional model of modern human origins: a reassessment of its morphological basis. *J. hum. Evol.* **26,** 23–56.

Lieberman, D. E. (1995). Testing hypotheses about recent human evolution from skulls. *Curr. Anthrop.* **36,** 159–197.

Maddison, D. R. (1991). African origin of human mitochondrial DNA reexamined. *Syst. Zool.* **40,** 355–363.

McBrearty, S. & Brooks, A. S. (2000). The revolution that wasn't: a new interpretation of the origin of modern human behavior. *J. hum. Evol.* **39,** 453–563.

Ovchinnikov, I. V., Götherström, A., Romanova, G. P., Kharitonov, V. M., Liden, K. & Goodwin, W. (2000). Molecular analysis of Neanderthal DNA from the northern Caucasus. *Nature* **404,** 490–493.

Page, S. L. & Goodman, M. (2001). Catarrhine phylogeny: non-coding DNA evidence for a diphyletic origin of mangabeys and for a human-chimpanzee clade. *Mol. Phylogenet. Evol.* **18,** 14–25.

Pilbeam, D. (1996). Genetic and morphological records of the Hominoidea and hominid origins: a synthesis. *Mol. Phylogenet. Evol.* **5,** 155–168.

Rightmire, G. P. (1990). *The Evolution of* Homo erectus. Cambridge: Cambridge University Press.

Ruvolo, M. (1997). Molecular phylogeny of the hominoids: inferences from multiple independent DNA data sets. *Mol. Biol. Evol.* **14,** 248–265.

Smith, F. H., Falsetti, A. B. & Donnelly, S. M. (1989). Modern human origins. *Yearb. phys. Anthrop.* **32,** 35–68.

Stringer, C. B. (1989). The origin of early modern humans: a comparison of the European and non-European evidence. In (P. Mellars & C. B. Stringer, Eds) *The Human Revolution: Behavioural and Biological Perspectives on the Origin of Modern Humans,* pp. 232–244. Edinburgh: Edinburgh University Press.

Stringer, C. B. (1992). Replacement, continuity and the origin of *Homo sapiens*. In (G. Braüer & F. H. Smith, Eds) *Continuity or Replacement? Controversies in* Homo sapiens *Evolution*, pp. 9–24. Rotterdam: Balkema.

Stringer, C. B. (2001). Modern human origins—distinguishing the models. *Afr. Archaeol. Rev.* **18,** 67–75.

Stringer, C. B. & Andrews, P. (1988). Genetic and fossil evidence for the origin of modern humans. *Science* **239,** 1263–1268.

Thorne, A. G. & Wolpoff, M. H. (1981). Regional continuity in Australian Pleistocene hominid evolution. *Am. J. phys. Anthrop.* **55,** 337–349.

Thorne, A. G. & Wolpoff, M. H. (1992). The multiregional evolution of modern humans. *Scient. Am.* **266,** 76–83.

Trinkaus, E. (1990). Cladistics and the hominid fossil record. *Am. J. phys. Anthrop.* **83,** 1–11.

Trinkaus, E. (1992). Cladistics and later Pleistocene human evolution. In (G. Braüer & F. H. Smith, Eds) *Continuity or Replacement? Controversies in* Homo sapiens *Evolution*, pp. 1–7. Rotterdam: Balkema.

Wolpoff, M. H. (1989). Multiregional evolution: the fossil alternative to Eden. In (P. Mellars & C. B. Stringer, Eds) *The Human Revolution: Behavioural and Biological Perspectives on the Origin of Modern Humans*, pp. 62–108. Edinburgh: Edinburgh University Press.

Wolpoff, M. H. (1992). Theories of modern human origins. In (G. Braüer & F. H. Smith, Eds) *Continuity or Replacement? Controversies in* Homo sapiens *Evolution*, pp. 25–63. Rotterdam: Balkema.

Wolpoff, M. H., Hawks, J. & Caspari, R. (2000). Multiregional, not multiple origins. *Am. J. phys. Anthrop.* **112,** 129–136.

Wolpoff, M. H., Hawks, J., Frayer, D. W. & Hunley, K. (2001). Modern human ancestry at the peripheries: a test of the replacement theory. *Science* **291,** 293–297.

Appendix 1. Details of the 96 qualitative craniodental characters used in the study

The description of each character is followed by the key to the character states (''States'') and the distribution of character states among the taxa (''Dist''). Further details, including the references for allocating the character states to the taxa, can be found in Collard & Wood (2000).

1. **Depth of subarcuate fossa**
   States: (0) deep; (1) moderately deep to shallow; (2) very shallow to nonexistent.
   Dist.: *Homo* 2; *Pan* 2; *Gorilla* 2; *Pongo* 2; *Hylobates* 1; *Colobus* 0.
2. **Morphology of the mandibular symphysis**
   States: (1) elongated and spout-like with an angle of 150°–145°; (2) symphysis with an angle of 137°–115°; (3) angle of mandibular symphysis (excluding the simian shelf) to horizontal ramus is narrow, approaching vertical when observed dorsally and laterally, with a mandibular symphysis angle of about 100°–90° or less.
   Dist.: *Homo* 3; *Pan* 2; *Gorilla* 1; *Pongo* 2; *Hylobates* 2; *Colobus* 1.
3. **Distinctiveness of angular process of mandible**
   States: (0) distinct, with posterior projection; (1) not distinct.
   Dist.: *Homo* 1; *Pan* 1; *Gorilla* 1; *Pongo* 1; *Hylobates* 0; *Colobus* 1.
4. **Direction of incisive (anterior palatine) foramen**
   States: (0) opening is directed dorsoventrally as in most mammals and the observer can see through the foramen; (1) foramen is directed diagonally, from anterior–ventral to posterior–dorsal, leads to a tube-like structure, and one cannot see through the foramina.
   Dist.: *Homo* 1; *Pan* 1; *Gorilla* 1; *Pongo* 1; *Hylobates* 0; *Colobus* 0.

5. **Carotid canal morphology when viewed from ventral side of cranium**
   States: (1) canal perforates bulla away from basicranium and is clearly within it, opening of canal is directed medially, ventrally or ventro-medially, but the imaginary lines (one from each side) which emerge from these openings do not cross at the foramen magnum, or cross at its anterior border at the level of the occipital condyles; (2) canal perforates bulla away from basicranium and is clearly within it, opening is directed postero-medially and the imaginary lines which emerge from these openings cross the foramen magnum posterior to the occipital condyles, or caudal to the foramen magnum itself.
   Dist.: *Homo* 1; *Pan* 1; *Gorilla* 1; *Pongo* 1; *Hylobates* 2; *Colobus* 1.
6. **Size of upper first incisor relative to upper second incisor**
   States: (0) about the same size; (1) enlarged; (2) much enlarged.
   Dist.: *Homo* 1; *Pan* 1; *Gorilla* 1; *Pongo* 2; *Hylobates* 0; *Colobus* 0.
7. **Honing in males (back of upper canine sharpens against third lower premolar).**
   States: (1) present, i.e., P_3 bilaterally compressed (sectorial) and modified for honing on C^1, P_3 is larger than P_4 especially mesiodistally, also may involve honing C^1 on C_1; (2) honing reduced, P_3 slightly buccolingually compressed, P_3 is larger than P_4 especially mesiodistally; (3) honing further reduced, P_3 about the same size as P_4 in length in occlusal view.
   Dist.: *Homo* 2; *Pan* 2; *Gorilla* 1; *Pongo* 1; *Hylobates* 1; *Colobus* 0.
8. **Interorbital pillar width.**
   States: (0) wide; (1) narrow.
   Dist.: *Homo* 0; *Pan* 0; *Gorilla* 0; *Pongo* 1; *Hylobates* 0; *Colobus* 0.
9. **Depth of middle ear**
   States: (0) shallow; (1) deepened, more than 8.5 mm.
   Dist.: *Homo* 1; *Pan* 1; *Gorilla* 1; *Pongo* 0; *Hylobates* 0; *Colobus* ?.
10. **Axis of ear bones**
    States: (0) acute angle; (1) right angle or more.
    Dist.: *Homo* 0; *Pan* 0; *Gorilla* 1; *Pongo* 1; *Hylobates* 1; *Colobus* ?.
11. **Area of inner ear**
    States: (0) low, <50 mm^2; (1) increased, >50 mm^2.
    Dist.: *Homo* 1; *Pan* 1; *Gorilla* 1; *Pongo* 0; *Hylobates* 0; *Colobus* ?.
12. **Klinorhynchy (a deep foreshortened facial skeleton which bends downward with respect to the cranial base)**
    States: (0) airorynch or straight; (1) more klinorhynch; (2) strongly klinorhynch.
    Dist.: *Homo* 2; *Pan* 2; *Gorilla* 2; *Pongo* 0; *Hylobates* 1; *Colobus* 0.
13. **Frontozygomatic suture**
    States: (0) vertical; (1) medially directed.
    Dist.: *Homo* 0; *Pan* 0; *Gorilla* 0; *Pongo* 1; *Hylobates* 0; *Colobus* 0.
14. **Relative height of upper face**
    States: (0) high, index about 70; (1) reduced.
    Dist.: *Homo* 1; *Pan* 0; *Gorilla* 0; *Pongo* 0; *Hylobates* 1; *Colobus* 0.
15. **Facial index (upper face height as a percentage of facial breadth)**
    States: (0) low, index about 50; (1) increased.
    Dist.: *Homo* 0; *Pan* 1; *Gorilla* 1; *Pongo* 1; *Hylobates* 0; *Colobus* 0.
16. **Height of mandibular symphysis relative to length of the lower toothrow**
    States: (0) low, its height about 60% of toothrow length; (1) deepened, at least 75% of tooth row length.
    Dist.: *Homo* 0; *Pan* 1; *Gorilla* 1; *Pongo* 1; *Hylobates* 0; *Colobus* 1.

17. Presence/absence of frontal sinus
States: (0) absent; (1) present.
Dist.: *Homo* 1; *Pan* 1; *Gorilla* 1; *Pongo* 0; *Hylobates* 0; *Colobus* 0.

18. Pyriform aperture
States: (0) narrow; (1) widened; (2) very wide.
Dist.: *Homo* 2; *Pan* 2; *Gorilla* 2; *Pongo* 1; *Hylobates* 2; *Colobus* 0.

19. Position of infraorbital foramina relative to zygomaxillary suture
States: (0) close to suture; (1) further from suture.
Dist.: *Homo* 0; *Pan* 0; *Gorilla* 0; *Pongo* 1; *Hylobates* 0; *Colobus* 1.

20. Orientation of zygomatic bone
States: (0) more frontally; (1) more superolaterally; (2) still further superolaterally.
Dist.: *Homo* 2; *Pan* 2; *Gorilla* 2; *Pongo* 1; *Hylobates* 0; *Colobus* 1.

21. Frontal bone
States: (0) flat; (1) more convex; (2) strongly convex.
Dist.: *Homo* 2; *Pan* 0; *Gorilla* 0; *Pongo* 2; *Hylobates* 1; *Colobus* 2.

22. Glabella prominence
States: (0) strong; (1) reduced; (2) absent.
Dist.: *Homo* 0; *Pan* 0; *Gorilla* 0; *Pongo* 1; *Hylobates* 2; *Colobus* 0.

23. Number of incisive foramina
States: (0) double, i.e., one on each side of the midline; (1) single, confluence of two foramina, at least close to the surface.
Dist.: *Homo* 1; *Pan* 0; *Gorilla* 0; *Pongo* 1; *Hylobates* 0; *Colobus* 0.

24. Maxillary sinus
States: (0) small; (1) expanded.
Dist.: *Homo* 0; *Pan* 0; *Gorilla* 0; *Pongo* 1; *Hylobates* 0; *Colobus* 0.

25. Supraorbital development
States: (0) weak; (1) more marked; (2) torus-like.
Dist.: *Homo* 2; *Pan* 2; *Gorilla* 2; *Pongo* 0; *Hylobates* 1; *Colobus* 1.

26. Supraorbital contour
States: (0) arched; (1) less arched.
Dist.: *Homo* 0; *Pan* 0; *Gorilla* 1; *Pongo* 0; *Hylobates* 0; *Colobus* 1.

27. Orbits
States: (0) as wide as high; (1) high oval.
Dist.: *Homo* 0; *Pan* 0; *Gorilla* 0; *Pongo* 1; *Hylobates* 0; *Colobus* 0.

28. Supraorbital trigon
States: (0) not developed; (1) developed.
Dist.: *Homo* 0; *Pan* 1; *Gorilla* 1; *Pongo* 1; *Hylobates* 0; *Colobus* 1.

29. Nasal width
States: (0) broad; (1) reduced.
Dist.: *Homo* 0; *Pan* 0; *Gorilla* 0; *Pongo* 1; *Hylobates* 0; *Colobus* 0.

30. Length of nasals
States: (0) long; (1) shortened.
Dist.: *Homo* 1; *Pan* 0; *Gorilla* 0; *Pongo* 0; *Hylobates* 1; *Colobus* 1.

31. Size of zygomatic foramina
States: (0) very small; (1) enlarged.
Dist.: *Homo* 0; *Pan* 0; *Gorilla* 0; *Pongo* 1; *Hylobates* 0; *Colobus* 0.

32. Position of zygomatic foramina
States: (0) at or below plane of orbital rim; (1) above plane of orbital rim.
Dist.: *Homo* 0; *Pan* 0; *Gorilla* 0; *Pongo* 1; *Hylobates* 0; *Colobus* 1.

33. Size of incisive foramina
States: (0) large; (1) reduced in size; (2) tiny.
Dist.: *Homo* 1; *Pan* 1; *Gorilla* 1; *Pongo* 2; *Hylobates* 0; *Colobus* 0.

34. Size and shape of palatine foramina
States: (0) large and wide; (1) small and narrow.
Dist.: *Homo* 0; *Pan* 0; *Gorilla* 0; *Pongo* 1; *Hylobates* 0; *Colobus* 0.

35. Premaxillary suture in adult
States: (0) patent; (1) obliterated.
Dist.: *Homo* 1; *Pan* 1; *Gorilla* 0; *Pongo* 0; *Hylobates* 0; *Colobus* 0.

36. Foramen lacerum medium
States: (0) absent; (1) present.
Dist.: *Homo* 1; *Pan* 0; *Gorilla* 0; *Pongo* 1; *Hylobates* 0; *Colobus* 1.

37. Posterior convergence of temporal lines
States: (0) converge posteriorly; (1) do not converge.
Dist.: *Homo* 1; *Pan* 0; *Gorilla* 0; *Pongo* 0; *Hylobates* 1; *Colobus* 1.

38. Mesial groove on male canine
States: (0) extends on to root; (1) present; (2) absent.
Dist.: *Homo* 1; *Pan* 1; *Gorilla* 1; *Pongo* 2; *Hylobates* 1; *Colobus* 0.

39. Relative height of male canine
States: (0) high relative to mesiodistal length; (1) lower relative to mesiodistal length.
Dist.: *Homo* 1; *Pan* 1; *Gorilla* 1; *Pongo* 1; *Hylobates* 0; *Colobus* 1.

40. Upper I2 occlusal edge
States: (0) slopes distally; (1) does not slope distally.
Dist.: *Homo* 1; *Pan* 1; *Gorilla* 0; *Pongo* 0; *Hylobates* 0; *Colobus* 0.

41. Robusticity of canines
States: (0) slender; (1) more robust.
Dist.: *Homo* 1; *Pan* 1; *Gorilla* 1; *Pongo* 1; *Hylobates* 0; *Colobus* 0.

42. Basal keel of lower canines
States: (0) present; (1) absent.
Dist.: *Homo* 1; *Pan* 1; *Gorilla* 0; *Pongo* 0; *Hylobates* 0; *Colobus* 0.

43. Basal area of paracone of upper premolars
States: (0) subequal to protocone; (1) smaller than protocone.
Dist.: *Homo* 0; *Pan* 0; *Gorilla* 0; *Pongo* 1; *Hylobates* 1; *Colobus* 1.

44. Molar cingulum
States: (0) prominent, shelf-like; (1) reduced, incomplete, (2) fragmented or absent.
Dist.: *Homo* 2; *Pan* 2; *Gorilla* 1; *Pongo* 2; *Hylobates* 1; *Colobus* 1.

45. Protoconid apex on lower dP3
States: (0) more lingual from the median axis; (1) truncated buccally from the median axis.
Dist.: *Homo* 1; *Pan* 0; *Gorilla* 0; *Pongo* 1; *Hylobates* 0; *Colobus* ?.

46. Metaconid of lower dP3
States: (0) present; (1) absent.
Dist.: *Homo* 0; *Pan* 1; *Gorilla* 1; *Pongo* 0; *Hylobates* 0; *Colobus* ?.

47. Protocristid of lower dP3
States: (0) aligned with tooth mesiodistal axis; (1) angled.
Dist.: *Homo* 1; *Pan* 0; *Gorilla* 0; *Pongo* 1; *Hylobates* 0; *Colobus* ?.

48. Talonid basin of lower dP3
States: (0) open distally; (1) closed.
Dist.: *Homo* 1; *Pan* 0; *Gorilla* 0; *Pongo* 1; *Hylobates* 0; *Colobus* ?.

49. Metaconid of lower dP4
States: (0) subequal to protoconid; (1) increased relative to protoconid on lower dP4.
Dist.: *Homo* 0; *Pan* 1; *Gorilla* 1; *Pongo* 0; *Hylobates* 0; *Colobus* ?.

50. Crista obliqua on lower dP4
States: (0) does not reach protoconid apex; (1) reaches protoconid apex.
Dist.: *Homo* 1; *Pan* 0; *Gorilla* 0; *Pongo* 1; *Hylobates* 1; *Colobus* ?.

51. Talonid basin on lower dP4
States: (0) open distally; (1) closed.
Dist.: *Homo* 1; *Pan* 0; *Gorilla* 0; *Pongo* 1; *Hylobates* 1; *Colobus* ?.

52. Protocone of upper dP3, in crown view
States: (0) larger than paracone; (1) smaller than paracone.
Dist.: *Homo* 1; *Pan* 0; *Gorilla* 0; *Pongo* 1; *Hylobates* 0; *Colobus* ?.

53. Preprotocrista of upper dP4
States: (0) weak; (1) more developed.
Dist.: *Homo* 1; *Pan* 1; *Gorilla* 1; *Pongo* 1; *Hylobates* 0; *Colobus* ?.

54. Postprotocrista of upper dP4
States: (0) poor; (1) more developed; (2) still more developed.
Dist.: *Homo* 2; *Pan* 2; *Gorilla* 2; *Pongo* 1; *Hylobates* 1; *Colobus* 0.

55. Protocristid grooves of molars
States: (0) prominent; (1) barely visible.
Dist.: *Homo* 0; *Pan* 1; *Gorilla* 0; *Pongo* 1; *Hylobates* 1; *Colobus* 0.

56. Lingual marginal ridges of molars
States: (0) hardly appreciable; (1) more prominent; (2) very prominent.
Dist.: *Homo* 1; *Pan* 1; *Gorilla* 2; *Pongo* 1; *Hylobates* 1; *Colobus* 0.

57. Thickness of molar enamel
States: (0) thin; (1) increased thickness; (2) very thick.
Dist.: *Homo* 2; *Pan* 0; *Gorilla* 0; *Pongo* 1; *Hylobates* 0; *Colobus* ?.

58. Proportion of Pattern 3 enamel
States: (0) high; (1) reduced; (2) very reduced.
Dist.: *Homo* 0; *Pan* 2; *Gorilla* 2; *Pongo* 1; *Hylobates* 0; *Colobus* ?.

59. Insertion of genioglossal
States: (0) above inferior transverse torus of internal (or posterior) mandibular symphysis; (1) shifted to inferior transverse torus.
Dist.: *Homo* 0; *Pan* 1; *Gorilla* 1; *Pongo* 1; *Hylobates* 0; *Colobus* 0.

60. Insertion of geniohyoideus
States: (0) basally on inferior transverse torus; (1) higher on inferior transverse torus; (2) above inferior transverse torus.
Dist.: *Homo* 2; *Pan* 2; *Gorilla* 1; *Pongo* 0; *Hylobates* 1; *Colobus* 0.

61. Insertion of digastric
States: (0) posterior to inferior transverse torus; (1) inferior transverse torus; (2) not on symphysis.
Dist.: *Homo* 1; *Pan* 1; *Gorilla* 0; *Pongo* 2; *Hylobates* 0; *Colobus* 0.

62. Encephalization
States: (0) low, <1.2; (1) increased, >1.2-1.9; (2) high >1.9.
Dist.: *Homo* 2; *Pan* 1; *Gorilla* 0; *Pongo* 1; *Hylobates* 2; *Colobus* 0.

63. Retroarticular canal
States: (0) absent; (1) present.
Dist.: *Homo* 0; *Pan* 0; *Gorilla* 0; *Pongo* 1; *Hylobates* ?; *Colobus* ?.

64. Condylar canal
States: (0) absent; (1) present.
Dist.: *Homo* 1; *Pan* 1; *Gorilla* 1; *Pongo* 0; *Hylobates* ?; *Colobus* ?.

65. Incisive fossa
States: (0) absent; (1) deep; (2) extends through palate.
Dist.: *Homo* 1; *Pan* 1; *Gorilla* 1; *Pongo* 0; *Hylobates* 2; *Colobus* ?.

66. Molar dentine horns
States: (0) high; (1) low.
Dist.: *Homo* 0; *Pan* 0; *Gorilla* 0; *Pongo* 1; *Hylobates* 0; *Colobus* ?.

67. Molar enamel wrinkling
States: (0) smooth or slight wrinkling; (1) deep secondary wrinkling.
Dist.: *Homo* 0; *Pan* 0; *Gorilla* 0; *Pongo* 1; *Hylobates* 0; *Colobus* ?.

68. Postorbital sulcus
States: (0) absent; (1) present.
Dist.: *Homo* 1; *Pan* 1; *Gorilla* 1; *Pongo* 0; *Hylobates* 0; *Colobus* ?.

69. Ethmoid-lacrymal contact
States: (0) long, 100%; (1) short, 40–90%.
Dist.: *Homo* 0; *Pan* 1; *Gorilla* 1; *Pongo* 0; *Hylobates* 0; *Colobus* ?.

70. Fronto-maxillary contact in orbits
States: (0) no contact; (1) contact, 30–50%.
Dist.: *Homo* 0; *Pan* 1; *Gorilla* 1; *Pongo* 0; *Hylobates* 0; *Colobus* ?.

71. Nasal floor morphology
States: (0) nasal floor stepped; (1) nasal floor unstepped.
Dist.: *Homo* 0; *Pan* 0; *Gorilla* 0; *Pongo* 1; *Hylobates* 0; *Colobus* ?.

72. Palatine fenestrae reduced in size
States: (0) no; (1) yes.
Dist.: *Homo* 1; *Pan* 1; *Gorilla* 1; *Pongo* 1; *Hylobates* 0; *Colobus* ?.

73. Cheek tooth height
States: (0) low; (1) medium; (2) medium-high; (3) high.
Dist.: *Homo* 0; *Pan* 2; *Gorilla* 3; *Pongo* 0; *Hylobates* 1; *Colobus* ?.

74. Lower M3 smaller than lower M2
States: (0) no; (1) yes.
Dist.: *Homo* 1; *Pan* 1; *Gorilla* 0; *Pongo* 1; *Hylobates* 1; *Colobus* ?.

75. Number of zygomatic foramina
States: (0) 1–2; (1) 1–2+.
Dist.: *Homo* 0; *Pan* 0; *Gorilla* 1; *Pongo* 1; *Hylobates* 0; *Colobus* ?.

76. Post talonid basin
States: (0) absent; (1) small; (2) narrow.
Dist.: *Homo* 1; *Pan* 2; *Gorilla* 2; *Pongo* 2; *Hylobates* 0; *Colobus* ?.

77. Relative depth of mandible
States: (0) deep/moderate; (1) moderate; (2) shallow.
Dist.: *Homo* 1; *Pan* 1; *Gorilla* 1; *Pongo* 1; *Hylobates* 2; *Colobus* 0.

78. Mandibular shape
States: (0) shallows mesially/constant; (1) constant; (2) deepens.
Dist.: *Homo* 1; *Pan* 1; *Gorilla* 1; *Pongo* 1; *Hylobates* 2; *Colobus* 0.

79. Ethmo-sphenoid contact
States: (0) none/very short, 0–39%; (1) short, 40–90%; (2) long, 91–100%.
Dist.: *Homo* 2; *Pan* 1; *Gorilla* 1; *Pongo* 2; *Hylobates* 0; *Colobus* ?.

80. Zygomatic bone
States: (0) curved; (1) flattened.
Dist.: *Homo* 0; *Pan* 0; *Gorilla* 0; *Pongo* 1; *Hylobates* 0; *Colobus* ?.

81. Relative face height
States: (0) 19–24; (1) 27–30.
Dist.: *Homo* 0; *Pan* 1; *Gorilla* 1; *Pongo* 1; *Hylobates* 0; *Colobus* ?.

82. Canine length as percentage of upper M1 (male)
States: (0) short, 61–81%; (1) longer, 101–182%.
Dist.: *Homo* 0; *Pan* 1; *Gorilla* 1; *Pongo* 1; *Hylobates* 1; *Colobus* ?.

83. Canine length as percentage of upper M1 (female)
States: (0) short, 61–81%; (1) longer, 92–144%.
Dist.: *Homo* 0; *Pan* 1; *Gorilla* 1; *Pongo* 1; *Hylobates* 1; *Colobus* ?.

84. Canine length as percentage of upper P4 (male)
States: (0) short, 116–160%; (1) longer, 215–543%.
Dist.: *Homo* 0; *Pan* 1; *Gorilla* 1; *Pongo* 1; *Hylobates* 1; *Colobus* ?.

85. Canine length as percentage of upper P4 (female)
States: (0) short, 116–178%; (1) longer, 187–273%; (2) still longer, 307–543%.
Dist.: *Homo* 0; *Pan* 1; *Gorilla* 0; *Pongo* ?; *Hylobates* 2; *Colobus* ?.

86. Angle between tooth rows
States: (0) low, − 5–16°+; (1) high, 20–40°.
Dist.: *Homo* 1; *Pan* 0; *Gorilla* 0; *Pongo* 0; *Hylobates* 0; *Colobus* ?.

87. Eruption after upper I2
States: (0) PCPM; (1) MPPC.
Dist.: *Homo* 0; *Pan* 1; *Gorilla* 1; *Pongo* 1; *Hylobates* 1; *Colobus* ?.

88. Eruption after lower I2
States: (0) CPPM; (1) MPPC.
Dist.: *Homo* 0; *Pan* 1; *Gorilla* 1; *Pongo* 1; *Hylobates* 1; *Colobus* ?.

89. Upper I1 lingual crenulations
States: (0) absent; (1) marginal; (2) whole surface.
Dist.: *Homo* 1; *Pan* 1; *Gorilla* 1; *Pongo* 2; *Hylobates* 1; *Colobus* ?.

90. Upper I1 cingulum tubercle
States: (0) present; (1) absent.
Dist.: *Homo* 0; *Pan* 1; *Gorilla* 1; *Pongo* 0; *Hylobates* 1; *Colobus* ?.

91. Number of upper I1 ridges
States: (0) one; (1) one or more than one; (2) always more than one.
Dist.: *Homo* 1; *Pan* 0; *Gorilla* 2; *Pongo* 1; *Hylobates* 0; *Colobus* ?.

92. Canine sexual dimorphism
States: (0) monomorphic; (1) dimorphic.
Dist.: *Homo* 0; *Pan* 1; *Gorilla* 1; *Pongo* 1; *Hylobates* 0; *Colobus* ?.

93. Canine elongation
States: (0) buccolingual; (1) none; (2) mesiodistal.
Dist.: *Homo* 0; *Pan* 2; *Gorilla* 2; *Pongo* 2; *Hylobates* 1; *Colobus* ?.

94. Lower P3 metaconid
States: (0) absent; (1) tiny; (2) small.
Dist.: *Homo* 2; *Pan* 0/1; *Gorilla* 1; *Pongo* 2; *Hylobates* 0; *Colobus* ?.

95. Trigonid basin
States: (0) narrow slit; (1) fair; (2) wider.
Dist.: *Homo* 1; *Pan* 2; *Gorilla* 2; *Pongo* 1; *Hylobates* 0; *Colobus* ?.

96. Sulcus obliqus
States: (0) weak to moderate definition; (1) strong to very strong definition.
Dist.: *Homo* 0; *Pan* 0; *Gorilla* 1; *Pongo* 1; *Hylobates* 0; *Colobus* ?.

Appendix 2. Details of the 171 soft-tissue characters used in the study.

The description of each character is followed by the key to the character states (''States'') and the distribution of character states among the taxa (''Dist''). Further details, including the references for allocating the character states to the taxa, can be found in Gibbs *et al.* (2002).

1. Omohyoid has three bellies in some specimens
States: 0=no, 1=yes
Dist.: *Hylobates* 0, *Pongo* 0, *Gorilla* 1, *Pan* 1, *Homo* 0

2. **Anterior bellies of digastric in contact in midline**
   States: 0=yes, 1=no
   Dist.: *Hylobates* 0, *Pongo* 0, *Gorilla* 1, *Pan* 0, *Homo* 1
3. **Cricothyroid insertion onto external surface of posterior thyroid lamina**
   States: 0=yes, 1=no
   Dist.: *Hylobates* 0, *Pongo* 1, *Gorilla* 1, *Pan* 0, *Homo* 1
4. **Shape of apex of tongue**
   States: 0=rounded, 1=square
   Dist.: *Hylobates* 0, *Pongo* 0, *Gorilla* 1, *Pan* 1, *Homo* 0
5. **Presence/absence of apical lingual gland**
   States: 0=absent, 1=variable, 2=present
   Dist.: *Hylobates* 0, *Pongo* 2, *Gorilla* 1, *Pan* 1, *Homo* 2
6. **Presence/absence of filiform papillae on posterior third of tongue**
   States: 0=present, 1=absent
   Dist.: *Hylobates* 0, *Pongo* 1, *Gorilla* 0, *Pan* 0, *Homo* 1
7. **Conical filiform predominate over cylindrical filiform**
   States: 0=yes, 1=no
   Dist.: *Hylobates* 0, *Pongo* 0, *Gorilla* 1, *Pan* 1, *Homo* 1
8. **Sublingual fold is triangular**
   States: 0=yes, 1=no
   Dist.: *Hylobates* 0, *Pongo* 1, *Gorilla* 0, *Pan* 0, *Homo* 1
9. **Abductor pollicis brevis divides into slips in some specimens**
   States: 0=no, 1=yes
   Dist.: *Hylobates* 0, *Pongo* 0, *Gorilla* 1, *Pan* 1, *Homo* 0
10. **Occasional reinforcement of abductor pollicis brevis by slips from flexor pollicis brevis**
    States: 0=yes, 1=no
    Dist.: *Hylobates* 0, *Pongo* 1, *Gorilla* 1, *Pan* 0, *Homo* 1
11. **Abductor pollicis brevis inserts into MI**
    States: 0=yes, 1=no
    Dist.: *Hylobates* 0, *Pongo* 1, *Gorilla* 0, *Pan* 0, *Homo* 1
12. **Radial head of flexor pollicis brevis originates from flexor retinaculum and trapezium only**
    States: 0=no, 1=yes
    Dist.: *Hylobates* 0, *Pongo* 0, *Gorilla* 1, *Pan* 1, *Homo* 1
13. **Site of origin of the humeral head of pronator teres**
    States: 0=medial humeral epicondyle, 1=medial humeral epicondyle and medial intermuscular septum
    Dist.: *Hylobates* 0, *Pongo* 1, *Gorilla* 0, *Pan* 1, *Homo* 1
14. **Humeral head of pronator teres fuses with flexor carpi radialis**
    States: 0=no, 1=yes
    Dist.: *Hylobates* 0, *Pongo* 1, *Gorilla* 0, *Pan* 1, *Homo* 0
15. **Humeroulnar head of flexor digitorum superficialis takes origin from intermuscular septum**
    States: 0=no, 1=yes
    Dist.: *Hylobates* 0, *Pongo* 0, *Gorilla* 1, *Pan* 1, *Homo* 1
16. **Flexor carpi radialis origin from intermuscular septum**
    States: 0=no, 1=yes
    Dist.: *Hylobates* 1, *Pongo* 0, *Gorilla* 0, *Pan* 1, *Homo* 1
17. **Flexor carpi radialis fused with flexor digitorum superficialis**
    States: 0=no, 1=yes
    Dist.: *Hylobates* 0, *Pongo* 1, *Gorilla* 1, *Pan* 1, *Homo* 0

18. Flexor carpi radialis insertion into palmar surface of base of MIII
States: 0=variable, 1=yes
Dist.: *Hylobates* ?, *Pongo* 0, *Gorilla* 1, *Pan* 0, *Homo* 1

19. Palmaris longus present in all specimens
States: 0=no, 1=yes
Dist.: *Hylobates* 1, *Pongo* 1, *Gorilla* 0, *Pan* 0, *Homo* 0

20. Flexor carpi ulnaris originates from intermuscular septum
States: 0=no, 1=yes
Dist.: *Hylobates* 0, *Pongo* 1, *Gorilla* 0, *Pan* 1, *Homo* 1

21. Flexor carpi ulnaris gives origin to some fibres of flexor digitorum superficialis
States: 0=no, 1=yes
Dist.: *Hylobates* 0, *Pongo* 1, *Gorilla* 0, *Pan* 1, *Homo* 0

22. Orientation of pronator quadratus
States: 0=strongly oblique, 1=moderately oblique, 2=weakly oblique
Dist.: *Hylobates* 0, *Pongo* 0, *Gorilla* 1, *Pan* 1, *Homo* 2

23. Origin of flexor digitorum profundus extends to medial coronoid process and/or medial humeral condyle
States: 0=no, 1=yes
Dist.: *Hylobates* 1, *Pongo* 0, *Gorilla* 1, *Pan* 0, *Homo* 1

24. Flexor pollicis longus originates from anterior radius and interosseous membrane
States: 0=no, 1=yes
Dist.: *Hylobates* 0, *Pongo* 0, *Gorilla* 1, *Pan* 1, *Homo* 1

25. Flexor pollicis longus takes origin from palmar fascia
States: 0=no, 1=yes
Dist.: *Hylobates* 0, *Pongo* 0, *Gorilla* 1, *Pan* 1, *Homo* 0

26. Flexor pollicis longus gives origin to tendon to digit II
States: 0=no, 1=occasionally, 2=often
Dist.: *Hylobates* 1, *Pongo* 0, *Gorilla* 0, *Pan* 2, *Homo* 1

27. Extensor carpi radialis brevis originates from radial collateral ligament
States: 0=no, 1=yes
Dist.: *Hylobates* 0, *Pongo* 1, *Gorilla* 0, *Pan* 1, *Homo* 1

28. Extensor carpi radialis brevis originates from intermuscular septum
States: 0=no, 1=yes
Dist.: *Hylobates* 0, *Pongo* 1, *Gorilla* 0, *Pan* 0, *Homo* 1

29. Extensor carpi radialis brevis inserts into MII
States: 0=yes, 1=variable, 2=no
Dist.: *Hylobates* 0, *Pongo* 2, *Gorilla* 0, *Pan* 2, *Homo* 1

30. Accessory tendon of extensor carpi radialis longus to MI
States: 0=no, 1=sometimes present (~10% specimens), 2=often present (~50% specimens)
Dist.: *Hylobates* 2, *Pongo* 0, *Gorilla* 0, *Pan* 0, *Homo* 1

31. Fusion of brachioradialis with brachialis
States: 0=yes, 1=variable, 2=no
Dist.: *Hylobates* 0, *Pongo* 2, *Gorilla* 2, *Pan* 0, *Homo* 1

32. Extensor digitorum originates from intermuscular septum
States: 0=no, 1=yes
Dist.: *Hylobates* 0, *Pongo* 1, *Gorilla* 0, *Pan* 1, *Homo* 1

33. Extensor digitorum commonly originates from forearm bones
States: 0=radius and ulna, 1=ulna only, 2=neither forearm bone
Dist.: *Hylobates* 1, *Pongo* 1, *Gorilla* 0, *Pan* 0, *Homo* 2

34. Extensor digitorum originates from antebrachial fascia
States: 0=no, 1=yes
Dist.: *Hylobates* 0, *Pongo* 0, *Gorilla* 0, *Pan* 1, *Homo* 1

35. Slips from extensor digitorum tendon for digit IV to digits III and V
States: 0=no, 1=yes
Dist.: *Hylobates* 0, *Pongo* 0, *Gorilla* 1, *Pan* 1, *Homo* 1

36. Coracobrachialis origination from intermuscular septum
States: 0=no, 1=variable, 2=yes
Dist.: *Hylobates* 0, *Pongo* 0, *Gorilla* 2, *Pan* 2, *Homo* 1

37. Coracobrachialis fused with brachialis
States: 0=no, 1=yes
Dist.: *Hylobates* 0, *Pongo* 1, *Gorilla* 1, *Pan* 1, *Homo* 0

38. Anterior extension of insertion of coracobrachialis present in most specimens
States: 0=no, 1=yes
Dist.: *Hylobates* 0, *Pongo* 0, *Gorilla* 1, *Pan* 1, *Homo* 1

39. Brachialis originates from septa
States: 0=no, 1=yes
Dist.: *Hylobates* 0, *Pongo* 1, *Gorilla* 1, *Pan* 0, *Homo* 1

40. Lateral head of triceps brachii originates from lateral intermuscular septum
States: 0=no, 1=yes
Dist.: *Hylobates* 0, *Pongo* 0, *Gorilla* 0, *Pan* 1, *Homo* 1

41. Extensor digitorum insertion extends into middle or distal phalanges in some specimens
States: 0=no, 1=yes
Dist.: *Hylobates* 0, *Pongo* 1, *Gorilla* 1, *Pan* 1, *Homo* 0

42. Extensor digitorum inserts into interphalangeal joints
States: 0=no, 1=yes
Dist.: *Hylobates* 0, *Pongo* 1, *Gorilla* 0, *Pan* 1, *Homo* 0

43. Extensor digiti minimi absent in some specimens
States: 0=no, 1=yes
Dist.: *Hylobates* 0, *Pongo* 1, *Gorilla* 0, *Pan* 1, *Homo* 1

44. Extension of extensor carpi ulnaris to first phalanx of digit V in some specimens
States: 0=no, 1=yes
Dist.: *Hylobates* 0, *Pongo* 0, *Gorilla* 0, *Pan* 1, *Homo* 1

45. Supinator origination from ligaments of elbow
States: 0=no, 1=yes
Dist.: *Hylobates* 0, *Pongo* 1, *Gorilla* 1, *Pan* 0, *Homo* 1

46. Abductor pollicis longus origination from intermuscular septum
States: 0=no, 1=yes
Dist.: *Hylobates* 0, *Pongo* 1, *Gorilla* 0, *Pan* 1, *Homo* 0

47. Extensor pollicis brevis origination from ulna and interosseous membrane
States: 0=no, 1=yes
Dist.: *Hylobates* 0, *Pongo* 0, *Gorilla* 1, *Pan* 1, *Homo* 1

48. Extensor pollicis brevis insertion onto base of proximal phalanx of digit I
States: 0=no, 1=yes
Dist.: *Hylobates* 0, *Pongo* 0, *Gorilla* 1, *Pan* 0, *Homo* 1

49. Extensor indicis origination from interosseous membrane
States: 0=yes, 1=no
Dist.: *Hylobates* 0, *Pongo* 0, *Gorilla* 1, *Pan* 1, *Homo* 0

50. Most common pattern of insertion of extensor indicis
States: 0=digits II, III and IV, 1=digits II and III, 2=digit II
Dist.: *Hylobates* 0, *Pongo* 1, *Gorilla* 2, *Pan* 2, *Homo* 2

51. Deltoid origination from infraspinous fascia
States: 0=no, 1=yes
Dist.: *Hylobates* 0, *Pongo* 1, *Gorilla* 0, *Pan* 1, *Homo* 0

52. Teres minor insertion extends onto shaft below greater tubercle
States: 0=no, 1=yes
Dist.: *Hylobates* 0, *Pongo* 0, *Gorilla* 1, *Pan* 1, *Homo* 1

53. Teres minor shares origin from intermuscular septum with teres major
States: 0=no, 1=yes
Dist.: *Hylobates* 0, *Pongo* 0, *Gorilla* 0, *Pan* 1, *Homo* 1

54. Latissimus dorsi may originate from inferior scapular angle
States: 0=no, 1=yes
Dist.: *Hylobates* 0, *Pongo* 0, *Gorilla* 0, *Pan* 1, *Homo* 1

55. Extent of costal origin of latissimus dorsi
States: 0=three or four ribs, 1=three, four or five ribs, 2=five ribs, 3=six ribs
Dist.: *Hylobates* 2, *Pongo* 3, *Gorilla* 3, *Pan* 1, *Homo* 0

56. Extent of origin of teres major from lateral scapular border
States: 0=30%, 1=50%, 2=more than 50%
Dist.: *Hylobates* 2, *Pongo* 0, *Gorilla* 0, *Pan* 1, *Homo* 0

57. Subscapularis insertion extends onto shaft below lesser humeral tubercle
States: 0=no, 1=yes
Dist.: *Hylobates* 0, *Pongo* 1, *Gorilla* 0, *Pan* 1, *Homo* 1

58. Accessory bundles of subscapularis present in some individuals
States: 0=no, 1=yes
Dist.: *Hylobates* 0, *Pongo* 1, *Gorilla* 0, *Pan* 1, *Homo* 1

59. Subclavius takes origin on first rib only
States: 0=no, 1=yes
Dist.: *Hylobates* 0, *Pongo* 0, *Gorilla* 1, *Pan* 1, *Homo* 1

60. Costal origin of serratus anterior extends to rib 12
States: 0=no, 1=yes
Dist.: *Hylobates* 0, *Pongo* 1, *Gorilla* 1, *Pan* 1, *Homo* 0

61. Cranial extent of costal origin of pectoralis major
States: 0=ribs one and two, 1=rib two only, 2=none
Dist.: *Hylobates* 2, *Pongo* 0, *Gorilla* 1, *Pan* 0, *Homo* 1

62. Caudal extent of costal origin of pectoralis major
States: 0=none, 1=rib eight
Dist.: *Hylobates* 0, *Pongo* 0, *Gorilla* 1, *Pan* 1, *Homo* 0

63. Extent of clavicular origin of pectoralis major
States: 0=two-thirds, 1=half, 2=third
Dist.: *Hylobates* 0, *Pongo* 2, *Gorilla* 2, *Pan* 1, *Homo* 1

64. Pectoralis major may divide into three parts
States: 0=no, 1=yes
Dist.: *Hylobates* 0, *Pongo* 1, *Gorilla* 0, *Pan* 1, *Homo* 1

65. Origin of psoas major extends to S1
States: 0=yes, 1=variable, 2=no
Dist.: *Hylobates* 0, *Pongo* 0, *Gorilla* 1, *Pan* 1, *Homo* 2

66. Coccygeus insertion into anococcygeal raphe
States: 0=yes, 1=no
Dist.: *Hylobates* 0, *Pongo* 1, *Gorilla* 0, *Pan* 1, *Homo* 1

67. Coccygeus insertion into sacrum
States: 0=no, 1=yes
Dist.: *Hylobates* 0, *Pongo* 0, *Gorilla* 1, *Pan* 0, *Homo* 1
68. Piriformis normally fused with gluteus medius
States: 0=yes, 1=no
Dist.: *Hylobates* 0, *Pongo* 0, *Gorilla* 1, *Pan* 1, *Homo* 1
69. Origin of gluteus minimus is continuous
States: 0=yes, 1=variable, 2=no
Dist.: *Hylobates* 0, *Pongo* 2, *Gorilla* 2, *Pan* 2, *Homo* 1
70. Gluteus medius origination from fascia lata
States: 0=no, 1=yes
Dist.: *Hylobates* 0, *Pongo* 1, *Gorilla* 1, *Pan* 1, *Homo* 0
71. Gluteus medius is bipennate
States: 0=no, 1=yes
Dist.: *Hylobates* 0, *Pongo* 0, *Gorilla* 1, *Pan* 1, *Homo* 0
72. Tensor fascia latae normally fused proximally with gluteus maximus
States: 0=yes, 1=no
Dist.: *Hylobates* 0, *Pongo* 0, *Gorilla* 0, *Pan* 1, *Homo* 1
73. Tensor fascia latae fused laterally with gluteus medius and minimus
States: 0=yes, 1=no
Dist.: *Hylobates* 0, *Pongo* 1, *Gorilla* 0, *Pan* 0, *Homo* 1
74. Gluteus maximus fused with biceps femoris
States: 0=no fusion, 1=at origin, 2=more distally
Dist.: *Hylobates* 1, *Pongo* 2, *Gorilla* 1, *Pan* 1, *Homo* 0
75. Gluteus maximus insertion into hypotrochanteric fossa
States: 0=no, 1=yes
Dist.: *Hylobates* 0, *Pongo* 1, *Gorilla* 1, *Pan* 1, *Homo* 0
76. Superior gemellus
States: 0=present, 1=variable, 2=absent
Dist.: *Hylobates* 2, *Pongo* 1, *Gorilla* 1, *Pan* 0, *Homo* 1
77. Quadratus femoris split at insertion
States: 0=yes, 1=variable, 2=no
Dist.: *Hylobates* 0, *Pongo* 0, *Gorilla* 2, *Pan* 1, *Homo* 2
78. Obturator externus fused at insertion with obturator internus
States: 0=yes, 1=variable, 2=no
Dist.: *Hylobates* 0, *Pongo* 1, *Gorilla* 1, *Pan* 0, *Homo* 2
79. Gracilis origin extends to whole pubic body
States: 0=yes, 1=no
Dist.: *Hylobates* 0, *Pongo* 1, *Gorilla* 0, *Pan* 0, *Homo* 1
80. Adductor brevis origination from superior pubic ramus
States: 0=no, 1=yes
Dist.: *Hylobates* 0, *Pongo* 1, *Gorilla* 1, *Pan* 1, *Homo* 0
81. Adductor brevis inserted between pectineus and upper part of adductor magnus
States: 0=yes, 1=no
Dist.: *Hylobates* 0, *Pongo* 1, *Gorilla* 1, *Pan* 1, *Homo* 0
82. Adductor magnus insertion into inferior border of quadratus femoris insertion
States: 0=yes, 1=no
Dist.: *Hylobates* 0, *Pongo* 0, *Gorilla* 1, *Pan* 1, *Homo* 1
83. Rectus femoris has two heads
States: 0=no, 1=variable, 2=yes
Dist.: *Hylobates* 0, *Pongo* 1, *Gorilla* 1, *Pan* 1, *Homo* 2

84. Vastus medialis origination from intermuscular septa
States: 0=no, 1=yes
Dist.: *Hylobates* 0, *Pongo* 1, *Gorilla* 0, *Pan* 0, *Homo* 1

85. Vastus medialis insertion onto medial patellar surface
States: 0=no, 1=variable, 2=yes
Dist.: *Hylobates* 0, *Pongo* 0, *Gorilla* 1, *Pan* 0, *Homo* 2

86. Vastus lateralis origination from iliofemoral ligament
States: 0=no, 1=yes
Dist.: *Hylobates* 0, *Pongo* 1, *Gorilla* 1, *Pan* 1, *Homo* 0

87. Articularis genus present
States: 0=yes, 1=variable
Dist.: *Hylobates* 0, *Pongo* 1, *Gorilla* 1, *Pan* 1, *Homo* 1

88. Origin of short head of biceps femoris
States: 0=posterolateral femur and lateral intermuscular septum, 1=posterolateral femur only
Dist.: *Hylobates* 0, *Pongo* 1, *Gorilla* 1, *Pan* 0, *Homo* 0

89. Long head of biceps femoris may insert into iliotibial tract
States: 0=no, 1=yes
Dist.: *Hylobates* 0, *Pongo* 1, *Gorilla* 1, *Pan* 1, *Homo* 0

90. Insertion of short head of biceps femoris onto lateral intermuscular septum
States: 0=no, 1=yes
Dist.: *Hylobates* 0, *Pongo* 1, *Gorilla* 0, *Pan* 1, *Homo* 0

91. Semitendinosus may share common origin with semimembranosus
States: 0=no, 1=yes
Dist.: *Hylobates* 0, *Pongo* 1, *Gorilla* 0, *Pan* 1, *Homo* 1

92. Semimembranosus inserts into popliteal fascia and posterior wall of knee capsule via oblique popliteal ligaments
States: 0=no, 1=yes
Dist.: *Hylobates* 0, *Pongo* 0, *Gorilla* 1, *Pan* 0, *Homo* 1

93. Tibialis anterior originates from crural fascia
States: 0=no, 1=yes
Dist.: *Hylobates* 0, *Pongo* 1, *Gorilla* 0, *Pan* 0, *Homo* 1

94. Extensor digitorum longus originates from crural fascia
States: 0=no, 1=yes
Dist.: *Hylobates* 0, *Pongo* 0, *Gorilla* 0, *Pan* 1, *Homo* 1

95. Incidence of peroneus tertius
States: 0=low incidence (0–5% of specimens), 1=moderate incidence (30–50% of specimens), 2=high incidence ($\sim$95% of specimens)
Dist.: *Hylobates* 1, *Pongo* 0, *Gorilla* 1, *Pan* 0, *Homo* 2

96. Peroneus longus origination from lateral tibial condyle
States: 0=yes, 1=no
Dist.: *Hylobates* 0, *Pongo* 1, *Gorilla* 1, *Pan* 0, *Homo* 0

97. Peroneus brevis may insert onto first and second phalanges of digit V
States: 0=no, 1=yes
Dist.: *Hylobates* 0, *Pongo* 0, *Gorilla* 1, *Pan* 1, *Homo* 1

98. Soleus often has tibial origin
States: 0=no, 1=yes
Dist.: *Hylobates* 0, *Pongo* 0, *Gorilla* 1, *Pan* 1, *Homo* 1

99. Plantaris often present
States: 0=no, 1=yes
Dist.: *Hylobates* 0, *Pongo* 0, *Gorilla* 0, *Pan* 1, *Homo* 1

100. Extensor digitorum brevis tendon to digit V normally present
States: 0=yes, 1=no
Dist.: *Hylobates* 0, *Pongo* 1, *Gorilla* 1, *Pan* 0, *Homo* 0

101. Slip from abductor hallucis into base of MI
States: 0=yes, 1=no
Dist.: *Hylobates* 0, *Pongo* 0, *Gorilla* 0, *Pan* 1, *Homo* 1

102. Both heads of flexor hallucis brevis fused with abductor hallucis
States: 0=yes, 1=no
Dist.: *Hylobates* 0, *Pongo* 1, *Gorilla* 1, *Pan* 0, *Homo* 1

103. Two heads of adductor hallucis fused
States: 0=yes, 1=variable, 2=no
Dist.: *Hylobates* 0, *Pongo* 2, *Gorilla* 2, *Pan* 1, *Homo* 0

104. Oblique head of adductor hallucis origination from sheath of peroneus longus
States: 0=no, 1=yes
Dist.: *Hylobates* 0, *Pongo* 1, *Gorilla* 0, *Pan* 1, *Homo* 1

105. Abductor hallucis may insert onto medial cuneiform
States: 0=no, 1=yes
Dist.: *Hylobates* 0, *Pongo* 0, *Gorilla* 0, *Pan* 1, *Homo* 1

106. Medial and lateral heads of flexor hallucis brevis separated by septum
States: 0=no, 1=yes
Dist.: *Hylobates* 0, *Pongo* 1, *Gorilla* 1, *Pan* 0, *Homo* 0

107. Origin of transverse head of adductor hallucis
States: 0=second and third metatarsophalangeal joints and ligaments, 1=second, third and fourth metatarsophalangeal joints and ligaments, 2=third, fourth and fifth metatarsophalangeal joints and ligaments
Dist.: *Hylobates* 1, *Pongo* 0, *Gorilla* 1, *Pan* 1, *Homo* 2

108. First dorsal interosseous originates from MI and MII
States: 0=no, 1=yes
Dist.: *Hylobates* 0, *Pongo* 0, *Gorilla* 0, *Pan* 1, *Homo* 1

109. Flexor digitorum brevis originates from plantar aponeurosis
States: 0=no, 1=yes
Dist.: *Hylobates* 0, *Pongo* 0, *Gorilla* 0, *Pan* 1, *Homo* 1

110. Flexor digitorum brevis may fuse with abductor hallucis
States: 0=no, 1=yes
Dist.: *Hylobates* 0, *Pongo* 1, *Gorilla* 0, *Pan* 1, *Homo* 0

111. Perforating veins in cubital fossa
States: 0=present, 1=variable, 2=absent
Dist.: *Hylobates* 0, *Pongo* 2, *Gorilla* 0, *Pan* 1, *Homo* 0

112. Basilic vein
States: 0=absent, 1=variable, 2=present
Dist.: *Hylobates* 0, *Pongo* 1, *Gorilla* 1, *Pan* 0, *Homo* 2

113. Cephalic vein limited to forearm
States: 0=no, 1=low incidence (20–25% of specimens), 2=high incidence (80–100% of specimens)
Dist.: *Hylobates* 0, *Pongo* 0, *Gorilla* 2, *Pan* 2, *Homo* 1

114. Palmar metacarpal arteries originate from deep palmar arch
States: 0=yes, 1=no
Dist.: *Hylobates* 0, *Pongo* 1, *Gorilla* 0, *Pan* 1, *Homo* 0

115. Origin of radialis indicus may include first palmar metacarpal artery
States: 0=no, 1=yes
Dist.: *Hylobates* 0, *Pongo* 0, *Gorilla* 1, *Pan* 1, *Homo* 1

116. Origin of posterior interosseous artery
Style: 0=brachial artery, 1=common interosseous
Dist.: *Hylobates* 0, *Pongo* 0, *Gorilla* 0, *Pan* 1, *Homo* 1

117. Dorsalis indicis and dorsal metacarpal branches of ulnar artery
States: 0=absent, 1=present
Dist.: *Hylobates* 0, *Pongo* 1, *Gorilla* 1, *Pan* 0, *Homo* 0

118. Termination of superficial palmar artery
States: 0=thenar muscles, 1=superficial palmar arch
Dist.: *Hylobates* 0, *Pongo* 1, *Gorilla* 0, *Pan* 1, *Homo* 1

119. Superficial palmar artery may pass over thenar muscles
States: 0=no, 1=yes
Dist.: *Hylobates* 0, *Pongo* 0, *Gorilla* 0, *Pan* 1, *Homo* 1

120. Origin of radial recurrent artery
States: 0=radial artery, 1=variable, 2=brachial artery
Dist.: *Hylobates* 0, *Pongo* 2, *Gorilla* 0, *Pan* 1, *Homo* 0

121. Dorsalis pollicis
States: 0=present, 1=absent
Dist.: *Hylobates* 0, *Pongo* 0, *Gorilla* 0, *Pan* 1, *Homo* 1

122. Point at which radial artery enters palm
States: 0=dorsum of second interosseous space, 1=dorsum of first interosseous space
Dist.: *Hylobates* 0, *Pongo* 0, *Gorilla* 1, *Pan* 1, *Homo* 1

123. Superior ulnar collateral artery may originate from brachial artery
States: 0=no, 1=yes
Dist.: *Hylobates* 0, *Pongo* 0, *Gorilla* 1, *Pan* 1, *Homo* 1

124. Profunda brachii may originate from brachial artery
States: 0=no, 1=yes
Dist.: *Hylobates* 1, *Pongo* 0, *Gorilla* 0, *Pan* 1, *Homo* 1

125. Lateral thoracic artery normally an independent branch of axillary artery
States: 0=no, 1=yes
Dist.: *Hylobates* 0, *Pongo* 0, *Gorilla* 1, *Pan* 1, *Homo* 1

126. Pectoral branch of thoracoacromial artery
States: 0=absent, 1=variable, 2=present
Dist.: *Hylobates* 0, *Pongo* 2, *Gorilla* 0, *Pan* 1, *Homo* 2

127. Superior thoracic artery
States: 0=absent, 1=present
Dist.: *Hylobates* 0, *Pongo* 0, *Gorilla* 1, *Pan* 1, *Homo* 1

128. Thyroidea ima may arise from left common carotid
States: 0=yes, 1=no
Dist.: *Hylobates* 0, *Pongo* 1, *Gorilla* 0, *Pan* 0, *Homo* 1

129. Most common form of branches from aortic arch is E (Keith, 1895)
States: 0=yes, 1=no
Dist.: *Hylobates* 1, *Pongo* 1, *Gorilla* 0, *Pan* 0, *Homo* 0

130. Perforating branch of peroneal artery anastomoses with anterior lateral malleolar artery
States: 0=yes, 1=no
Dist.: *Hylobates* 0, *Pongo* 1, *Gorilla* 1, *Pan* 0, *Homo* 0

131. Peroneal artery takes origin from posterior tibial artery
States: 0=yes, 1=no
Dist.: *Hylobates* 0, *Pongo* 1, *Gorilla* 0, *Pan* 1, *Homo* 0

132. Digital branches of deep plantar arch to adjacent sides of digits II and III
States: 0=present, 1=variable, 2=absent
Dist.: *Hylobates* 0, *Pongo* 2, *Gorilla* 0, *Pan* 1, *Homo* 0

133. Lateral plantar artery dominant
States: 0=no, 1=variable, 2=yes
Dist.: *Hylobates* 0, *Pongo* 0, *Gorilla* 2, *Pan* 1, *Homo* 2

134. Inferior medial and inferior lateral genicular branches of popliteal artery
States: 0=present, 1=absent
Dist.: *Hylobates* 0, *Pongo* 1, *Gorilla* 1, *Pan* 0, *Homo* 0

135. Medial femoral circumflex artery may originate from profunda femoris
States: 0=no, 1=yes
Dist.: *Hylobates* 0, *Pongo* 0, *Gorilla* 0, *Pan* 1, *Homo* 1

136. Three or more perforating branches of profunda femoris
States: 0=no, 1=yes
Dist.: *Hylobates* 0, *Pongo* 0, *Gorilla* 1, *Pan* 0, *Homo* 1

137. Muscular branches of profunda femoris for hamstrings
States: 0=no, 1=yes
Dist.: *Hylobates* 0, *Pongo* 0, *Gorilla* 0, *Pan* 1, *Homo* 1

138. Muscular branches of profunda femoris for quadriceps
States: 0=no, 1=yes
Dist.: *Hylobates* 0, *Pongo* 1, *Gorilla* 0, *Pan* 1, *Homo* 1

139. Number of digits supplied by median nerve
States: 0=normally two and a half, 1=normally three and a half
Dist.: *Hylobates* 0, *Pongo* 0, *Gorilla* 1, *Pan* 1, *Homo* 1

140. Number of digits supplied by radial nerve
States: 0=normally one and a half, 1=normally two and a half
Dist.: *Hylobates* 0, *Pongo* 0, *Gorilla* 1, *Pan* 0, *Homo* 1

141. Gangliform enlargement at junction of radial and posterior interosseous nerves
States: 0=no, 1=yes
Dist.: *Hylobates* 0, *Pongo* 0, *Gorilla* 0, *Pan* 1, *Homo* 1

142. Axillary nerve innervates subscapularis
States: 0=no, 1=yes
Dist.: *Hylobates* 0, *Pongo* 1, *Gorilla* 1, *Pan* 0, *Homo* 0

143. Origin of axillary nerve
States: 0=C5–7, 1=C5–8, 2=C5–8 and T1
Dist.: *Hylobates* 1, *Pongo* 1, *Gorilla* 2, *Pan* 2, *Homo* 0

144. Number of lumbricals innervated by ulnar nerve
States: 0=normally one, 1=normally two, 2=normally three
Dist.: *Hylobates* 1, *Pongo* 1, *Gorilla* 2, *Pan* 0, *Homo* 1

145. Ulnar nerve may innervate flexor pollicis brevis
States: 0=no, 1=yes
Dist.: *Hylobates* 0, *Pongo* 1, *Gorilla* 0, *Pan* 1, *Homo* 1

146. Ulnar nerve normally supplies hypothenar muscles
States: 0=no, 1=yes
Dist.: *Hylobates* 0, *Pongo* 1, *Gorilla* 0, *Pan* 1, *Homo* 1

147. Origin of subscapular nerves
States: 0=C5, C6, 1=C5–7, 2=C5–8, 3=C5–8 and T1
Dist.: *Hylobates* 2, *Pongo* 1, *Gorilla* 3, *Pan* 3, *Homo* 0

148. Psoas minor innervated by femoral nerve
States: 0=no, 1=yes
Dist.: *Hylobates* 0, *Pongo* 0, *Gorilla* 1, *Pan* 1, *Homo* 1

149. Lateral cutaneous nerve of thigh may originate from L1 and L2
States: 0=no, 1=yes
Dist.: *Hylobates* 0, *Pongo* 1, *Gorilla* 0, *Pan* 1, *Homo* 0

150. Femoral nerve origination
States: 0=L2–4, 1=variable (L2–4 or L1–3), 2=L1–3
Dist.: *Hylobates* 0, *Pongo* 2, *Gorilla* 0, *Pan* 1, *Homo* 0

151. Genitofemoral nerve origination from L2
States: 0=yes, 1=no
Dist.: *Hylobates* 0, *Pongo* 1, *Gorilla* 0, *Pan* 1, *Homo* 0

152. Genitofemoral nerve may pass lateral to psoas major
States: 0=no, 1=yes
Dist.: *Hylobates* 0, *Pongo* 0, *Gorilla* 1, *Pan* 1, *Homo* 0

153. Obturator nerve origination from L1
States: 0=no, 1=yes
Dist.: *Hylobates* 0, *Pongo* 1, *Gorilla* 0, *Pan* 1, *Homo* 0

154. Muscular branches of obturator nerve may include pectineus
States: 0=no, 1=yes
Dist.: *Hylobates* 0, *Pongo* 0, *Gorilla* 0, *Pan* 1, *Homo* 1

155. Muscular branches of medial plantar nerve
States: 0=one medial lumbrical, 1=two medial lumbricals, 2=two medial lumbricals and adductor hallucis
Dist.: *Hylobates* 1, *Pongo* 2, *Gorilla* 0, *Pan* 2, *Homo* 0

156. Number of digital branches of lateral plantar nerve
States: 0=one and a half, 1=two and a half
Dist.: *Hylobates* 0, *Pongo* 1, *Gorilla* 1, *Pan* 1, *Homo* 0

157. Muscular branches of tibial nerve includes flexor digitorum longus
States: 0=no, 1=yes
Dist.: *Hylobates* 0, *Pongo* 0, *Gorilla* 1, *Pan* 1, *Homo* 1

158. Superficial peroneal nerve supplies medial side of digit II
States: 0=yes, 1=no
Dist.: *Hylobates* 0, *Pongo* 0, *Gorilla* 0, *Pan* 1, *Homo* 1

159. Average body hair density
States: 0=high, 1=moderate, 2=low
Dist.: *Hylobates* 0, *Pongo* 1, *Gorilla* 1, *Pan* 2, *Homo* 2

160. Sternal glands
States: 0=present, 1=absent
Dist.: *Hylobates* 0, *Pongo* 0, *Gorilla* 1, *Pan* 1, *Homo* 1

161. Ratio of nipple position to horizontal height index of nipple position
States: 0=2.6, 1=1.7–1.8, 2=1.0–1.1
Dist.: *Hylobates* 0, *Pongo* 2, *Gorilla* 1, *Pan* 1, *Homo* 2

162. Axillary organ
States: 0=absent, 1=present
Dist.: *Hylobates* 0, *Pongo* 0, *Gorilla* 1, *Pan* 1, *Homo* 1

163. Bulbospongiosus origination from ischial ramus
States: 0=yes, 1=no
Dist.: *Hylobates* 0, *Pongo* 1, *Gorilla* 0, *Pan* 0, *Homo* 1

164. Bulbospongiosus origination from perineal body
States: 0=no, 1=variable, 2=yes
Dist.: *Hylobates* 0, *Pongo* 2, *Gorilla* 1, *Pan* 0, *Homo* 2

165. Penile spines normally present
States: 0=yes, 1=no
Dist.: *Hylobates* 0, *Pongo* 1, *Gorilla* 1, *Pan* 0, *Homo* 1

166. Ventral groove in glans penis
States: 0=present, 1=absent
Dist.: *Hylobates* 0, *Pongo* 1, *Gorilla* 0, *Pan* 1, *Homo* 1

167. Scrotum normally postpenial
States: 0=no, 1=yes
Dist.: *Hylobates* 0, *Pongo* 0, *Gorilla* 0, *Pan* 1, *Homo* 1

168. Dependency of scrotum
States: 0=nondependent, 1=nondependent or semi-dependent, 2=semi-dependent or dependent, 3=dependent
Dist.: *Hylobates* 1, *Pongo* 0, *Gorilla* 0, *Pan* 2, *Homo* 3

169. Relative testes size (ratio of observed/predicted body testes size)
States: 0=<0.4, 1=>0.4
Dist.: *Hylobates* 0, *Pongo* 0, *Gorilla* 0, *Pan* 1, *Homo* 1

170. Urethral papilla
States: 0=present, 1=absent
Dist.: *Hylobates* 0, *Pongo* 1, *Gorilla* 0, *Pan* 1, *Homo* 1

171. Transverse rugae of vagina
States: 0=little developed, 1=well developed
Dist.: *Hylobates* 0, *Pongo* 0, *Gorilla* 1, *Pan* 1, *Homo* 1

Appendix 3. Details of the 129 craniodental quantitative characters used in the study

Further details can be found in Collard & Wood (2000).

Character	Definition
P1	I^1 labiolingual diameter
P2	I^1 mesiodistal diameter
P3	I^2 labiolingual diameter
P4	I^2 mesiodistal diameter
P5	C^1 mesiodistal diameter
P6	C^1 labiolingual diameter
P7	C^1 labial height
P8	P^3 buccolingual diameter
P9	P^3 mesiodistal diameter
P10	P^4 buccolingual diameter
P11	P^4 mesiodistal diameter
P12	M^1 buccolingual diameter
P13	M^1 mesiodistal diameter
P14	M^2 buccolingual diameter
P15	M^2 mesiodistal diameter
P16	M^3 buccolingual diameter
P17	M^3 mesiodistal diameter
P18	Outer alveolar breadth at M^3
P19	Inter upper canine breadth
P20	Palate length
P21	Inner alveolar breadth at M^3
P22	Palate depth at M^1
P23	Prosthion to plane of M^3
P24	Maxillo-Alveolar breadth (M^2B-M^2 B)
P25	Breadth between upper second molars (M^2L-M^2L)
P26	Palate depth at incisive fossa
P27	Palate depth at upper second molars
P28	Maxillary alveolar subtense
P29	Upper incisor alveolar length
P30	Upper premolar alveolar length
P31	Upper molar alveolar length
M1	I_1 labiolingual diameter
M2	I_1 mesiodistal diameter
M3	I_2 labiolingual diameter
M4	I_2 mesiodistal diameter
M5	C_1 labiolingual diameter
M6	C_1 mesiodistal diameter
M7	C_1 labial height
M8	P_3 buccolingual diameter
M9	P_3 mesiodistal diameter
M10	P_4 buccolingual diameter
M11	P_4 mesiodistal diameter
M12	M_1 buccolingual diameter
M13	M_1 mesiodistal diameter
M14	M_2 buccolingual diameter
M15	M_2 mesiodistal diameter
M16	M_3 buccolingual diameter
M17	M_3 mesiodistal diameter
M18	Maximum cusp height
M19	Condylar height
M20	Bicondylar breadth

M21	Coronoid height
M22	Bicoronoid breadth
M23	Right condylar head width
M24	Right condylar head anterior-posterior breadth
M25	Ramal breadth
M26	Bigonial width
M27	Height of mandibular body at M_1
M28	Thickness of mandibular body of M_1
M29	Symphyseal height
M30	Symphyseal thickness
M31	Inner alveolar breadth at M_3
M32	Maximum mandibular length
M33	Inter lower canine distance
M34	Mandibular corpus height at M_3
M35	Height of foramen spinosum
M36	Height of mental foramen
M37	Breadth between lower second molars
M38	Lower incisor alveolar length
M39	Lower premolar alveolar length
M40	Lower molar alveolar length
F1	Right orbital breadth
F2	Right orbital height
F3	Interorbital breadth
F4	Biorbital breadth
F5	Nasion–Rhinion
F6	Nasion–nasospinale
F7	Maximum nasal width
F8	Nasospinale–Prosthion
F9	Bijugal breadth
F10	Bizygomatic breadth
F11	Upper facial breadth
F12	Lower facial breadth
F13	Breadth between infraorbital foramina
F14	Lower nasal bone breadth
F15	Facial height
F16	Height of infraorbital foramen
F17	Height of orbital margin
F18	Upper malar height
F19	Lower malar height
F20	Upper facial prognathism
F21	Lower facial prognathism
F22	Malar prognathism
F23	Naso-frontal subtense
F24	Maxillary subtense
C1	Glabella–opisthocranion
C2	Minimum post-orbital breadth
C3	Basion-Bregma
C4	Maximum bi-parietal breadth
C5	Biporionic width
C6	Mastoid length
C7	Coronale-Coronale
C8	Opisthion-Inion
C9	Bimastoid width
C10	Posterior skull length
C11	Breadth across tympanic plates
C12	Breadth between carotid canals
C13	Breadth between petrous apices
C14	Breadth between foramen ovale
C15	Breadth between infratemporal crests
C16	Breadth of mandibular fossa
C17	Length of tympanic plate
C18	Length of petrous temporal
C19	Position of foramen ovale
C20	Position of infratemporal crest
C21	Length of foramen magnum
C22	Breadth of foramen magnum
C23	Length of infratemporal fossa
C24	Breadth of infratemporal fossa
C25	Opisthion–infratemporal subtense
C26	Basiooccipital length
C27	Parietal thickness at Lambda
C28	Frontal sagittal chord
C29	Parietal sagittal chord
C30	Parietal coronal chord
C31	Occipital sagittal chord
C32	Frontal sagittal arc
C33	Occipital sagittal arc
C34	Auricular height